AD-A157 926 STATISTICAL EVALUATION OF FORECASTS OVER THE LOW-LATITUDES(U) AIR FORCE INST OF TECH WRIGHT-PATTERSON AFB OH C P ZELZER AUG 85 1/1

UNCLASSIFIED F/G 4/2 NL

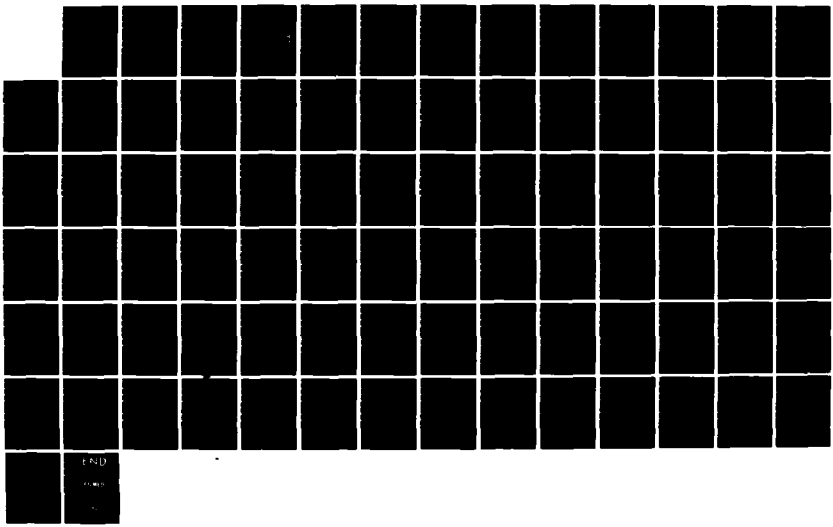

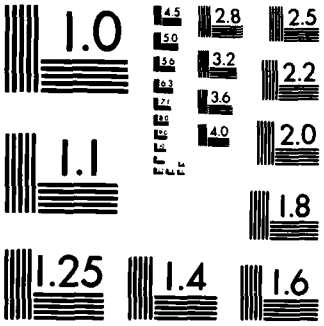

MICROCOPY RESOLUTION TEST CHART
NATIONAL BUREAU OF STANDARDS-1963-A

AD-A157 926

DTIC FILE COPY

THE FLORIDA STATE UNIVERSITY

COLLEGE OF ARTS AND SCIENCES

Statistical Evaluation of Forecasts over the Low-Latitudes

by

Christopher Paul Zelzer

A Thesis submitted to the
Department of Meteorology in
partial fulfillment of the
requirements for the degree
Master of Science

Approved:

Professor Directing Thesis

This document has been approved
for public release and sale;
distribution is unlimited.

August, 1985

UNCLASS

SECURITY CLASSIFICATION OF THIS PAGE (When Data Entered)

REPORT DOCUMENTATION PAGE

READ INSTRUCTIONS BEFORE COMPLETING FORM

1. REPORT NUMBER: AFIT/CI/NR 85-80T

2. GOVT ACCESSION NO.: A157926

3. RECIPIENT'S CATALOG NUMBER:

4. TITLE (and Subtitle): Statistical Evaluation of Forecasts over the Low-Latitudes

5. TYPE OF REPORT & PERIOD COVERED: THESIS/DISSERTATION

6. PERFORMING ORG. REPORT NUMBER:

7. AUTHOR(s): Christopher Paul Zelzer

8. CONTRACT OR GRANT NUMBER(s):

9. PERFORMING ORGANIZATION NAME AND ADDRESS: AFIT STUDENT AT: The Florida State University

10. PROGRAM ELEMENT, PROJECT, TASK AREA & WORK UNIT NUMBERS:

11. CONTROLLING OFFICE NAME AND ADDRESS: AFIT/NR, WPAFB OH 45433

12. REPORT DATE: August 1985

13. NUMBER OF PAGES: 70

14. MONITORING AGENCY NAME & ADDRESS (if different from Controlling Office):

15. SECURITY CLASS. (of this report): UNCLASS

15a. DECLASSIFICATION/DOWNGRADING SCHEDULE:

16. DISTRIBUTION STATEMENT (of this Report): APPROVED FOR PUBLIC RELEASE; DISTRIBUTION UNLIMITED

17. DISTRIBUTION STATEMENT (of the abstract entered in Block 20, if different from Report):

18. SUPPLEMENTARY NOTES: APPROVED FOR PUBLIC RELEASE: IAW AFR 190-1

Lynn Wolaver
LYNN E. WOLAVER
Dean for Research and Professional Development
AFIT, Wright-Patterson AFB OH

5 AUG 1985

19. KEY WORDS (Continue on reverse side if necessary and identify by block number):

20. ABSTRACT (Continue on reverse side if necessary and identify by block number):

ATTACHED

DD FORM 1 JAN 73 1473 EDITION OF 1 NOV 65 IS OBSOLETE

UNCLASS

SECURITY CLASSIFICATION OF THIS PAGE (When Data Entered)

85 8 13 075

FOLD DOWN ON OUTSIDE - SEAL WITH TAPE

AFIT/NR
WRIGHT-PATTERSON AFB OH 45433

OFFICIAL BUSINESS
PENALTY FOR PRIVATE USE, $300

NO POSTAGE
NECESSARY
IF MAILED
IN THE
UNITED STATES

BUSINESS REPLY MAIL
FIRST CLASS PERMIT NO. 73236 WASHINGTON D.C.

POSTAGE WILL BE PAID BY ADDRESSEE

AFIT/ DAA
Wright-Patterson AFB OH 45433

FOLD IN

AFIT RESEARCH ASSESSMENT

The purpose of this questionnaire is to ascertain the value and/or contribution of research accomplished by students or faculty of the Air Force Institute of Technology (AU). It would be greatly appreciated if you would complete the following questionnaire and return it to:

AFIT/NR
Wright-Patterson AFB OH 45433

RESEARCH TITLE: Statistical Evaluation of Forecasts over the Low-Latitudes

AUTHOR: Christopher Paul Zelzer

RESEARCH ASSESSMENT QUESTIONS:

1. Did this research contribute to a current Air Force project?

( ) a. YES ( ) b. NO

2. Do you believe this research topic is significant enough that it would have been researched (or contracted) by your organization or another agency if AFIT had not?

( ) a. YES ( ) b. NO

3. The benefits of AFIT research can often be expressed by the equivalent value that your agency achieved/received by virtue of AFIT performing the research. Can you estimate what this research would have cost if it had been accomplished under contract or if it had been done in-house in terms of manpower and/or dollars?

( ) a. MAN-YEARS _____ ( ) b. $_____

4. Often it is not possible to attach equivalent dollar values to research, although the results of the research may, in fact, be important. Whether or not you were able to establish an equivalent value for this research (3. above), what is your estimate of its significance?

( ) a. HIGHLY SIGNIFICANT ( ) b. SIGNIFICANT ( ) c. SLIGHTLY SIGNIFICANT ( ) d. OF NO SIGNIFICANCE

5. AFIT welcomes any further comments you may have on the above questions, or any additional details concerning the current application, future potential, or other value of this research. Please use the bottom part of this questionnaire for your statement(s).

NAME GRADE POSITION

ORGANIZATION LOCATION

STATEMENT(s):

COPY INSPECTED 2

Accession For
NTIS
DTIC
Unannounced
Justification
By
Distribution/
Availability Codes
Avail and/or
Dist Special
A-1

ABSTRACT

A series of experiments, designed to study single level predictions with a barotropic and a primitive equation model has been carried out for 15 June to 15 September 1979 utilizing FGGE (First GARP Global Experiment) data sets. The level chosen for this study is 700 mb with two separate domains being covered. Domain 1 covered a region from 120°W to 75°W and 20°S to 40°N, while Domain 2 covered a region from 75°W to 30°W and 20°S to 45°N. This study includes a discussion of tropical storm Claudette and also an analysis of the predictions using root mean square vector wind errors and absolute correlations. The results of 93 experiments show that the simple model based on the conservation of vorticity performs worse than persistence for all time periods in Domain 1 and 2. The model based on the conservation of potential vorticity performs better than persistence for up to 1 day in Domain 1, and up to 4 days in Domain 2. Past experiments and performance are compared. These included the following regions: the Atlantic and West Africa during the northern summer; a region including the Indian Ocean, Indonesia and the central Pacific Ocean during the northern winter; and a similar region during the northern summer. In general, useful skill of all the regions considered is exhibited only over the following: Central America and South America during northern summer to 4 days, West Africa and Eastern Atlantic during northern summer to 4 days, Central Pacific Ocean during northern winter to 1 day.

ACKNOWLEDGMENTS

The author would like to express his appreciation for the guidance and support provided by Professor T.N. Krishnamurti throughout this research. Acknowlegdments are also made to N.E. LaSeur and C.L. Jordan for their suggestions regarding this thesis.

Gratitude is also due to my colleagues in the Room 410 laboratory for their support and suggestions and special thanks to Ms. Brenda Weil for her excellent typing of the manuscript.

TABLE OF CONTENTS

	Page
ABSTRACT	ii
ACKNOWLEGEMENT	iii
TABLE OF CONTENTS	iv
LIST OF ILLUSTRATIONS	vi
LIST OF TABLES	viii
LIST OF ACRONYMS	ix
LIST OF SYMBOLS	x
1. Introduction	1
2. The Models	4
2.1 Filtered barotropic model	4
2.1.1 Basic equations	4
2.1.2 Features of the barotropic model	5
2.2 One-level PE model	7
2.2.1 Basic equations	7
2.2.2 Features of the one-level PE model	8
2.2.3 Boundary conditions	8
2.2.4 Treatment of the height of the mean free surface, $\bar{z}$	10
2.2.5 Initialization	11
3. Tropical Storm Claudette	12
4. Results of prediction experiments over the Atlantic Ocean and the Caribbean Sea	40
4.1 Verification - Region 1	43
4.2 Verification - Region 2	43
4.3 Flow field representation	46
4.4 Representative weather regimes on model performance	53

Page

5. Results of past predictive experiments 56
   5.1 The Atlantic Ocean and Western Africa 59
   5.2 The summer monsoon 60
   5.3 The winter monsoon 60

6. Summary and conclusions 64

APPENDIX A 67

REFERENCES 69

LIST OF ILLUSTRATIONS

Figure		Page
3.1	Path of Claudette. Positions are marked as of 1200 GMT on the indicated days. Closed circles indicate periods of development	13
3.2	Observed streamlines at 700 mb on 13 July at 1200 GMT	14
3.3	700 mb streamlines valid 14 July, 1200 GMT. (a) observation (b) barotropic (c) PE 24 hour forecast	15
3.4	700 mb streamlines valid 15 July, 1200 GMT (a) observation (b) barotropic (c) PE 24 hour forecast	18
3.5	700 mb isotachs valid 15 July, 1200 GMT. (a) observation (b) barotropic (c) PE 24 hour forecast	20
3.6	700 mb streamlines valid 16 July, 1200 GMT. (a) observation (b) barotropic (c) PE 24 hour forecast	22
3.7	700 mb streamlines valid 17 July, 1200 GMT. (a) observation (b) barotropic (c) PE 24 hour forecast	24
3.8	700 mb streamlines valid 18 July, 1200 GMT. (a) observation (b) barotropic (c) PE 24 hour forecast	27
3.9	700 mb streamlines valid 21 July, 1200 GMT. (a) observation (b) barotropic (c) PE 24 hour forecast	29
3.10	700 mb streamlines valid 22 July, 1200 GMT. (a) observation (b) barotropic (c) PE 24 hour forecast	31

Figure | Page

3.11 700 mb isotachs valid 22 July, 1200 GMT. (a) observation (b) barotropic (c) PE 24 hour forecast 33

3.12 700 mb streamlines valid 23 July, 1200 GMT. (a) observations (b) barotropic (c) PE 24 hour forecast 35

3.13 700 mb isotachs valid 23 July, 1200 GMT. (a) observations (b) barotropic (c) PE 24 hour forecast 38

4.1 Domain of numerical forecasts. Region I comprises an area of 120°W-75°W, 20.625°S-39.375°N and Region II an area of 75°W-30°W, 20.625°S-39.375°N 42

4.2 (a) to (m) refers to streamline analysis characteristics which often lead to good forecasts (a) is the observation for 30 June, 1979 at 1200 GMT. (b), (c) and (d) are the 24 hour observation and the barotropic and one-level PE predictions respectively. (e), (f), (g); (h), (i), (j); and (k), (l), (m) are the same as (b), (c), (d) but for the 48, 72, and 96 hours respectively 48

4.3 Streamline analysis showing typical characteristics which often lead to poor forecasts (a) observed rotational winds (b) observed total winds (rotational and divergent) 55

5.1 Domain of numerical forecasts. Areas are as in Table 4. (a) Regions III, IV and V, (b) Regions VI and VII 57

LIST OF TABLES

Tables | Page

CHAPTER 2:

1. Table 1a: Typical domain invariants of the barotropic model 9

Table 1b: Typical domain invariants of the PE model 9

CHAPTER 4:

2. Table 2: Root mean square errors of forecast wind errors, valid 13 Aug. at 700 mb. Values are averaged over area and number of forecasts. Units are ms^{-1} 41

3. Table 3a: Root mean square error of forecast wind errors at 700 mb for Region I. Values are averaged over area and number of forecasts. Units are ms^{-1} 44

Table 3b: Same as Table 3a except for Region II 45

Table 3c: Absolute correlation coefficients between forecast and observed winds at 700 mb for Region I. Values are averaged over number of forecasts 47

CHAPTER 5:

4. Table 4: Root mean square errors of forecast wind errors. Regions I and II were discussed in Chapter 4 and are included for comparison. Domains are shown in Figs. 4.1 and 5 63

LIST OF ACRONYMS

FGGE	First GARP Global Experiment
GARP	Global Atmospheric Reserach Program
GATE	GARP Atlantic Tropical Experiment
GMT	Greenwich Mean Time
RMS	Root Mean Square
PE	Primitive Equation
ECMWF	European Center for Medium Range Weather Forecast
GTDL	Geophysical Fluid Dynamics Laboratory
TOS	Tropical Observing System

LIST OF SYMBOLS

c	phase speed
f	earth's vorticity
g	earth's gravity
h	terrain height
u	zonal wind component
v	meridional wind component
z	free surface height
J	Jacobian operator
β	meridional deviation of the earth's vorticity
ζ	relative vorticity
ζ_a	absolute vorticity
ζ_p	potential vorticity
ψ	streamfunction
E_T	total energy parameter

CHAPTER 1

Introduction

The use and study of simple barotropic models is appealing on several levels. Since the equatorial tropics is generally dominated by barotropic dynamics, a barotropic model could be expected to display a reasonable level of skill over the region. In addition, the physical processes included in these models are very basic, requiring a simple and straight forward explanation of the models performance. The determination of a simple model's performance provides the basis for further development. Other uses of the barotropic models have been demonstrated by Shapiro (1977), who has suggested the non-linear terms in the balance vorticity equation may be used as a criterion for the development of a tropical depression. Shapiro has found the non-linear terms become significant prior to intensification. Barotropic models have also been used as prediction models for tropical storm tracks by Sanders et al. (1975, 1980). Sanders uses the conservation of absolute vorticity, the basic mechanism of barotropic prediction, as an explanation of the apparent steering of the storm vortex by larger scale flow within which the storm is

embedded. The relative importance of advective effects, such vorticity advection, and non-advective effects, such as divergence, can be inspected through the use of barotropic models.

The two models used in this study are a non-divergent barotropic and a divergent barotropic model. The 700 mb pressure surface level has been chosen as a good approximation of the non-divergent level over the tropics. In addition, African waves have been noted as having their maximum amplitude near 700mb. The data for the forecasts were obtained from the FGGE Level IIIb data.

Evaluation of the reliability of FGGE III-b data sets by Julian (1981) suggests that the Tropical Observing System (TOS) is capable of resolving the medium and large-scale divergent windfield. Large-scale dynamic features present an excellent inverse relationship of divergent/convergent flow between upper and lower levels, which also match with satellite depiction of strong convection. However, the objective analysis schemes are not able to treat adequately strong divergence/convergence fields on scales smaller than about 6-8 degrees latitude. Quantitative analysis of the root mean square difference of the analyzed minus the observed rawinsonde winds yield values near 3 mps. On a subjective basis, the analysis does a credible job on the tropical wind field: continuity is good in time as well as in the vertical dimension. Some specific areas of analysis which may be

questionable can be noted by large difference between ECMWF and GFDL analyses (Lau, 1984). Examples include data sparse areas, such as over oceans; divergent components depicted 50% higher by GFDL than ECMWF, including the Hadley circulations; and transports of westerly momentum stronger by ECMWF analyses than by GFDL.

Chapter 2 contains the basics of the barotropic and primitive equation (PE) models used for the forecasts. In Chapter 3, tropical storm Claudette is traced from the African coast through the Gulf of Mexico and into Texas. Chapter 4 discusses the statistical results of 93 forecasts during the period 15 July to 15 September 1979 and a brief review of other studies is included in Chapter 5.

CHAPTER 2

The models

2.1 Filtered barotropic model.

2.1.1 Basic equations.

The filtered barotropic model uses the principle of conservation of absolute vorticity, $\frac{d}{dt}(\zeta + f) = 0$, where ζ is the relative vorticity and f is the Coriolis parameter. Future values of relative vorticity are determined, from which the new flow field may be calculated. Since only the rotational part of the wind is included in the model, the streamfunction, ψ, may be used, where $u = -\frac{\partial\psi}{\partial y}$ and $v = \frac{\partial\psi}{\partial x}$. Thus the horizontal flow field may be represented as

$$V_H = k \times \nabla\psi$$

and the vorticity as

$$\zeta = \frac{\partial^2\psi}{\partial x^2} + \frac{\partial^2\psi}{\partial y^2} = \nabla^2\psi \qquad (1)$$

This allows the conservation of absolute vorticity to be rewritten as

$$\frac{\partial}{\partial t} C^2\psi = -J(\psi,\nabla^2\psi) - \beta\frac{\partial\psi}{\partial x} \qquad (2)$$

where $\beta = \frac{df}{dy}$ and J is the Jacobian operator which handles the advective process. A list of symbols is provided in Table 1.

2.1.2 Features of the barotropic model.

This model, in addition to conservation of absolute vorticity, also conserves mean vorticity, mean square vorticity and mean kinetic energy. The use of finite differences and a limited number of grid points also limits the resolution of the model, allowing only a limited number of waves to be represented. Aliasing results when wavelengths outside of these limits are misrepresented as allowable waves. In addition, nonlinear instability arises if the intersection of two waves produces a wave number identical to one of the original. Repetition of this feedback can quickly cause an increase in energy in short wavelengths.

A solution to this problem in the Arakawa Jacobian, where the advection of the vorticity ζ by the rotational part of the wind ψ may be written as

$$J(\psi,\zeta) = \frac{1}{3}\left\{J_1(\psi,\zeta) + J_2(\psi,\zeta) + J_3(\psi,\zeta)\right\} \quad (3)$$

where the three Jacobians on the right hand side of the equation are three alternate expressions of the advective terms:

$$\begin{aligned} J_1(\psi,\zeta) &= \frac{\partial\psi}{\partial x}\frac{\partial\zeta}{\partial y} - \frac{\partial\psi}{\partial y}\frac{\partial\zeta}{\partial x} \\ J_2(\psi,\zeta) &= \frac{\partial}{\partial y}\,\zeta\,\frac{\partial\psi}{\partial x} - \frac{\partial}{\partial x}\,\zeta\,\frac{\partial\psi}{\partial y} \\ J_3(\psi,\zeta) &= \frac{\partial}{\partial x}\,\psi\,\frac{\partial\zeta}{\partial y} - \frac{\partial}{\partial y}\,\psi\,\frac{\partial\zeta}{\partial x} \end{aligned} \quad (4)$$

The Arakawa Jacobian eliminates the false production of mean square vorticity and mean kinetic energy by insuring that interactions of these between adjacent grid points is exactly canceled. With the mean square vorticity and mean kinetic energy conserved, and thus the average wave number, the continued growth of very short waves is prevented.

An Euler forward-backward time differencing scheme following Matsuno (1970) is used. This is a two-step predictor-corrector which damps energy slightly. The predictor can be written as

$$P'_{t+\Delta t} = P_t + Q_t \Delta t \tag{5}$$

where $\frac{\partial P}{\partial t} = Q$. The corrector is

$$P_{t+\Delta T} = P_t + Q'_{t+\Delta t} \Delta t \tag{6}$$

The time differencing is used with a time step of 3600 seconds and a grid spacing of 1.875 degrees. As usual, the Courant, Levy, Fredrich criterion, $\Delta t < \frac{\Delta x}{|c + U_{max}|}$ determined values to insure stability. A standard second order Laplacian is used and the Poisson's equation for the streamfunction is solved by the use of relaxation. Two different boundary conditions have been used to limit the extent of the domain. The zonal direction has been extended by adding six extra grid points beyond the original domain and simple linear interpolation has been used to smooth the region. This has in effect removed the east and west boundaries, producing a continuity of the analysis in a cyclic

sense. The north and south bounderies were treated differently. The initial streamfunction is made to vary in the zonal direction while the tendency of the streamfunction, $\frac{\partial \psi}{\partial t}$ is set to zero at the two boundaries during integration. The effect is of an open boundary with u, v = constant at the north and south boundaries. The conditions at the north and south boundaries actually cause the invariants to not be completely conserved. The invariants are calculated for each day of every 96 hour forecast and an example is presented in Table 1a. The variance is small, typically within 10%, and previous results have shown open boundaries to be superior to results gained from closed boundaries.

2.2 One-level PE model

The one-level primitive equation model (PE) uses the u and v wind components directly without a conversion to the streamfunction. This model is an improvement upon the filtered barotropic model since the divergent flow is now part of the model.

2.2.1 Basic equation

The model is described by the following equations:

The equation of motion:

$$\frac{Du}{Dt} = fv - g \frac{\partial}{\partial x}(z+h) \tag{7}$$

$$\frac{Dv}{Dt} = -fu - g \frac{\partial}{\partial y}(z+h) \tag{8}$$

Mass continuity equation:

$$\frac{Dz}{Dt} = -z \left[\frac{\partial u}{\partial x} + \frac{\partial v}{\partial y}\right] \tag{9}$$

where z is the height of the free surface and h is a smoothed terrain height.

2.2.2 Features of the one-level PE model

Parcel invariants included in the model are the potential vorticity, $\zeta_p = \frac{(\zeta + f)}{z}$ and all its powers, $\zeta_p{}^n$. The domain invariants include the average potential vorticity, $\overline{\zeta_p}$, and all its powers $\overline{\zeta_p{}^n}$; the total energy, $E_T = z\ K + \frac{gz}{2} + gh$; and the mean height of the free surface, $\overline{z}$. An example is presented in Table 1b. Since open boundaries were used due to the limited domain size, total invariance of these properties is not to be expected. However, as with the barotropic model, the variance is small, usually within 3%, and open boundaries provide superior results compared to those of closed boundaries.

A semi-Langrangian advection scheme according to Krishnamurti (1962) and Mathur(1970) is used for horizontal advection. This method avoids the actual calculation of the non-linear terms by determining at time t the position of the parcel which will arrive at a specific grid point at the future time of $t + \Delta t$. The predicted value is simply taken to be the value of that parcel at time t. This method allows stable advection of the non-linear terms while at the same time allowing for the domain invariants.

2.2.3 Boundary conditions

The boundary conditions include adding a cyclic region to

TABLE 1A: Typical domain invariants of the barotropic model

30 JUN	$\overline{\zeta a}$ (s^{-1})	$\overline{\zeta_a}^2$ (s^{-2})
0 hours	2.20×10^{-5}	1.95×10^{-9}
24 hours	2.25×10^{-5}	1.97×10^{-9}
48 hours	2.13×10^{-5}	1.99×10^{-9}
72 hours	2.13×10^{-5}	2.07×10^{-9}
96 hours	2.26×10^{-5}	2.21×10^{-9}

TABLE 1B: Typical domain invariants of the PE model

30 JUN	$\overline{\zeta_p}$ $(m^{-1}s^{-1})$	$\overline{\zeta_p}^2$ $(m^{-2}s^{-2})$
0 hours	1.125×10^{-6}	5.188×10^{-15}
24 hours	1.112×10^{-6}	5.013×10^{-15}
48 hours	1.110×10^{-6}	5.002×10^{-15}
72 hours	1.110 c 10^{-6}	5.011×10^{-15}
96 hours	1.109×10^{-6}	5.012×10^{-15}

the east boundary of the domain. This region is created using the original u and v fields, while the geopotential is obtained as usual from the non-linear balance equation. The north and south boundaries are open, however, $\frac{\partial v}{\partial t} = \frac{\partial u}{\partial t} = 0$. Since u and v remain constant throughout the iterations, large discontinuities may develop. These are handled by a smoothing function which treats the second row of grid points away from both the north and south boundaries,

$$F_{ij} = \alpha\ (F_{ij}) + 1/2(1-\alpha)(F_{ij} + F_{ij-1}) \qquad (10)$$

where F is the variable and α is a smoothing coefficient = 0.95.

2.2.4 Treatment of the height of the mean free surface, z.

The height of the mean free surface is important since the height of the free surface is made up of the sum of a mean and a perturbation,

$$z = \bar{z} + z' \qquad (11)$$

The importance of the mean height of the surface can be seen by the wave phase speed relation

$$c = u \pm \sqrt{gz} \qquad (12)$$

where c is the wave phase speed. An alternate view of the importance of the height of the free surface can be seen in the mass continuity equation (eq. 9). This indicates that a reduction in the free surface height should reduce the effect of divergence or convergence, and thus of negative or positive vorticity changes, upon the height tendency. Williamson (1976) has shown that values of z smaller than the actual mean value tend to slow the

waves down and improve the forecasts. A mean free height of 2000m (Krishnamurti et al. 1979a) is used in an attempt to produce realistic wave speeds. The bottom topography h of the region (Gates and Nelson, 1975) further provides realistic flows. This topography has been interpolated to a 1.875° grid mesh. Additionally, a modification in the terrain heights is also required to produce realistic wave phase speeds, especially over higher elevations. This is accomplished by

$$h_{modified} = (h_{original}) \times \frac{1500}{h_{max}}$$

where h_{max} is the maximum height of the original smoothed terrain.

2.2.5 Initialization

Dynamic initialization is used to adjust the u, v and z fields to a state characteristic of the atmosphere. This is done in order to discourage spurious gravity waves from destroying the quality of the forecast. A forward and backward integration of the model causes the generation of inertial gravity waves in areas of imbalance. This results in a redistribution of the motion and pressure fields. The integration of the model continues for 18 iterations and results in a wind-pressure balance which is consistent with the dynamics of the one-level model.

CHAPTER 3

Tropical Storm Claudette

This section will trace the history of an African wave as it crosses the Atlantic and twice develops into tropical storm Claudette (Fig. 3.1). Claudette left the African coast as the strongest wave at midtropospheric levels of the 1979 season. The wave developed into a tropical storm for two brief periods separated by a five day interval in which it weakened into a disorganized tropical wave. Claudette never reached hurricane intensity, but did pass over Puerto Rico, Hispaniola, and southeast Texas. The result was one of the wettest tropical cyclones to affect the United States, including a record 42 inches of rainfall in 24 hours recorded by an observer near Alvin, Texas. Claudette eventually would cause one death by drowning and produce $400 million worth of flood damage, the tenth costliest tropical cyclone in United States history.

Claudette left the African coast on 12 July 1979 and is first present within the forecast region by 13 July 1979 (fig. 3.2). The 24 hour forecst for both models, valid on 14 July, moves the wave quickly west. The relative forecasts of the barotropic and PE models are compared in Fig. 3.3 The barotropic

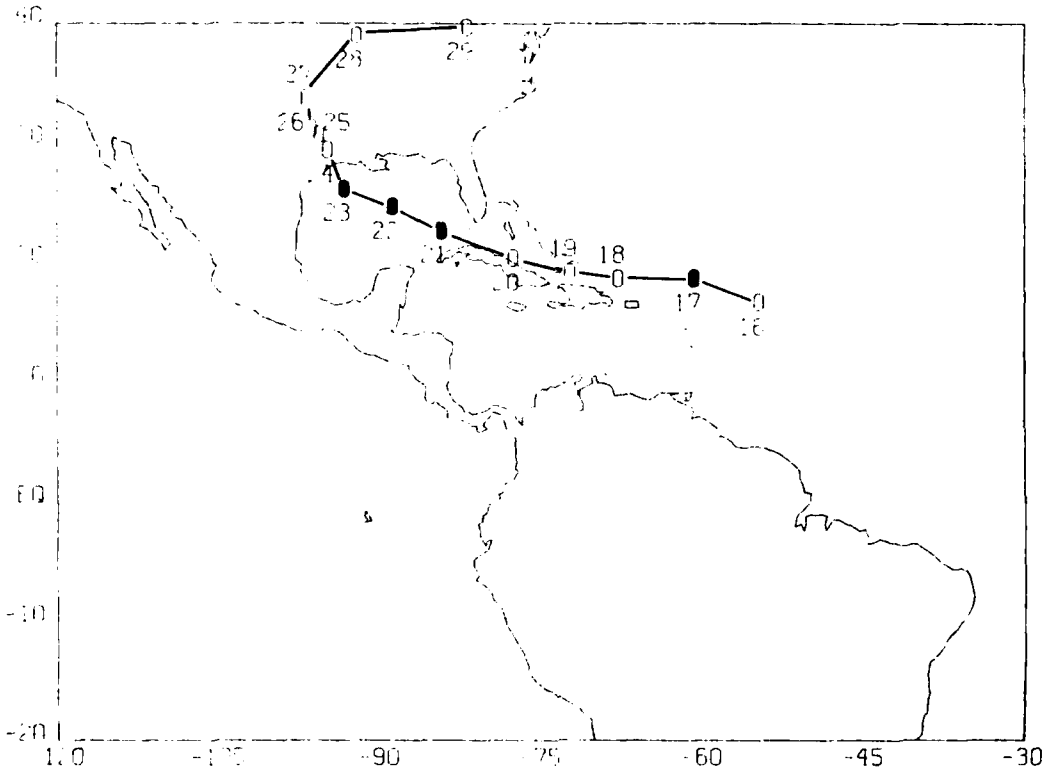

FIGURE 3.1 Path of Claudette. Positions are marked as of 1200 GMT on the indicated days. Closed circles indicate periods of development

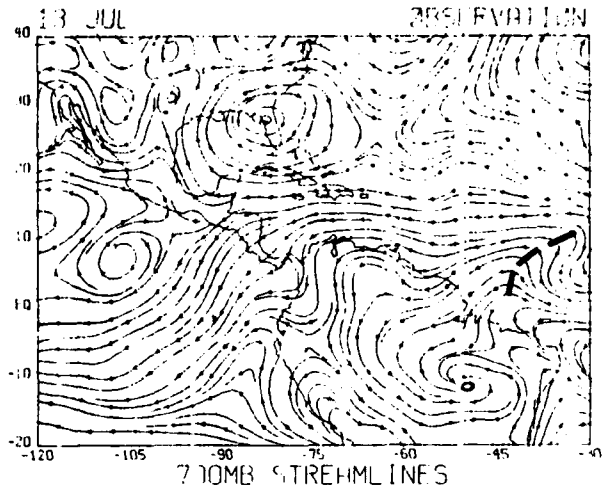

FIGURE 3.2 Observed streamlines at 700 mb on 13 July at 1200 GMT

FIGURE 3.3 700 mb streamlines valid 14 July, 1200 GMT. (a) observation (b) barotropic (c) PE 24 hour forecast

a

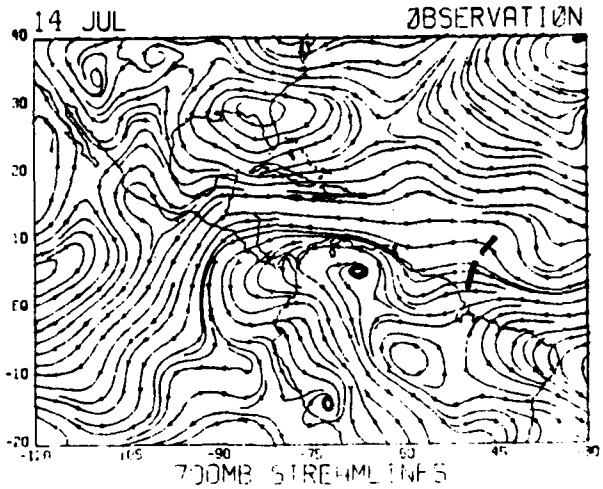
14 JUL
ØBSERVATIØN
700MB STREAMLINES

b

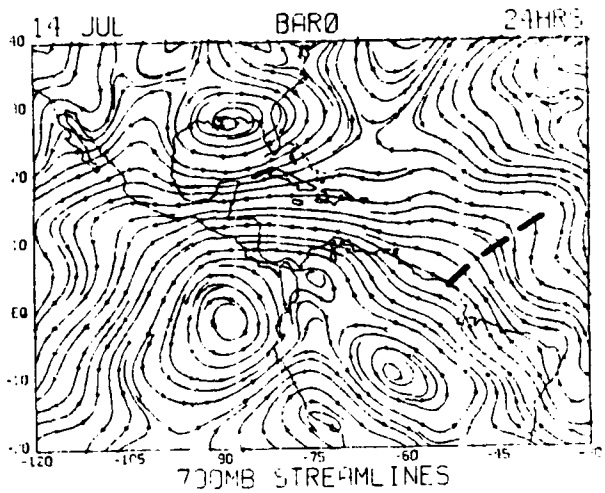
14 JUL
BARØ
24HRS
700MB STREAMLINES

c

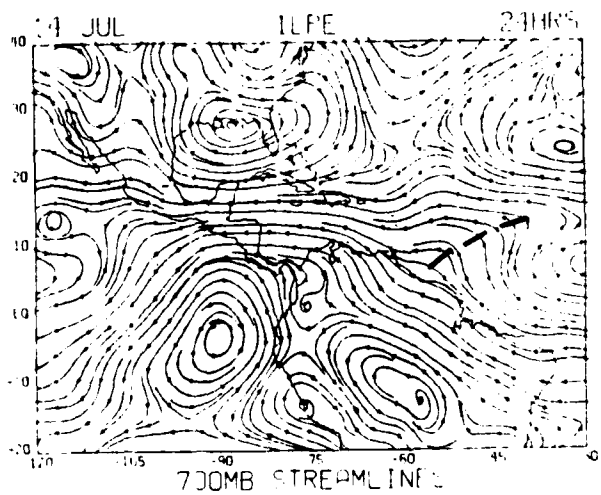
14 JUL
ILPE
24HRS
700MB STREAMLINES

24 hour wave phase speed is very good, although the actual identity of the wave became confused to the north. The PE model kept the identity of the wave separate, however it moved the wave 4-6° too fast while increasing the eastward tilt. Figs. 3.4 and 3.5 compare the wave positions and isotachs valid on 15 July. Once again the barotropic model does very well forecasting the wave phase speed but errs by continuing to increase the amplitude of the wave. The barotropic model has also underforecast the wind speed by about 4 mps. The PE model overdevelops the wave amplitude and again exaggerates the eastward tilt of the wave, however, the forecast wind speeds are accurate.

The period between 15 July and 19 July illustrates one of the problems encountered by a one-level model. Within this period, the wave begins to first lose intensity, and then later develops into a tropical depression. Surface circulations were first evident on 16 July and the wave was upgraded to tropical storm Claudette at 1600GMT 17 July. Through this period, the models never forecast the development or decay of the wave. One example begins on 16 July (Fig. 3.6). The amplitude of the wave is nearly nonexistent, and the 24 hour forecast continues with rather undisturbed flow. The actual flow field valid on 17 July is quite different (Fig. 3.7), the wave now is showing a distinct, large amplitude disturbance. After 17 July, both one-level models now forecast closed circulation at 700mb with little movement of the system. The 18 July observation shows a very

FIGURE 3.4 700 mb streamlines valid 15 July, 1200 GMT (a) observation (b) barotropic (c) PE 24 hour forecast

a

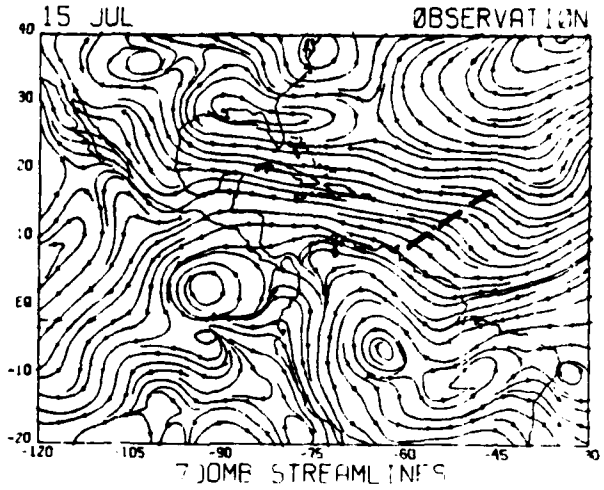
15 JUL
ØBSERVATION
40
30
20
10
EQ
-10
-20
-120
-105
-90
-75
-60
-45
30
700MB STREAMLINES

b

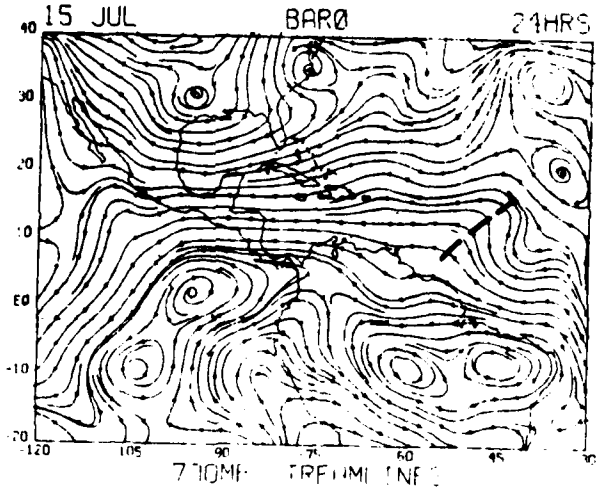
15 JUL
BARØ
24HRS
40
30
20
10
EQ
-10
-20
-120
-105
-90
-75
-60
-45
30

c

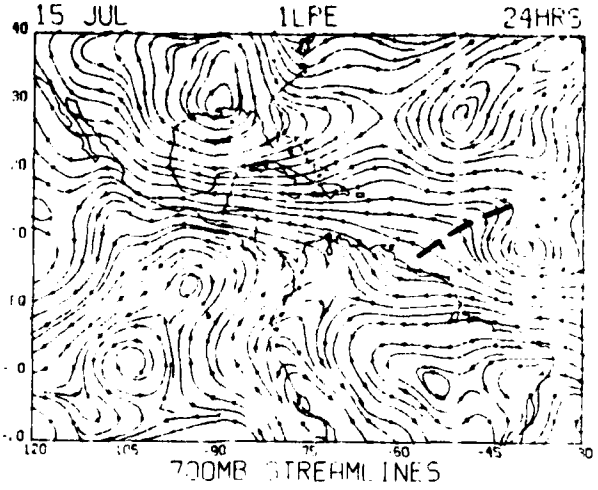
15 JUL
ILPE
24HRS
40
30
-120
-105
-90
-75
-60
-45
30
700MB STREAMLINES

FIGURE 3.5 700 mb isotachs valid 15 July, 1200 GMT. (a) observation (b) barotropic (c) PE 24 hour forecast

a

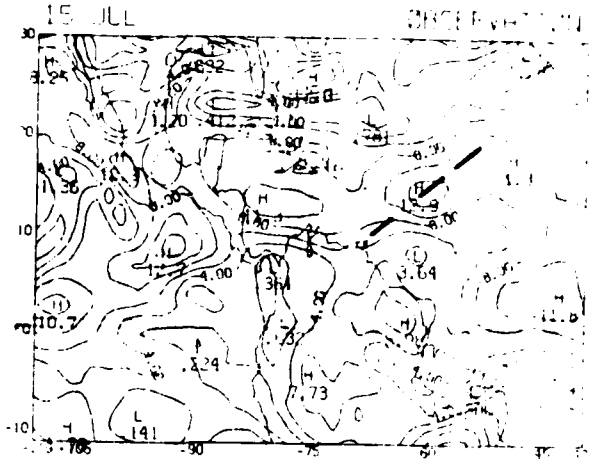

ISØTACHS

b

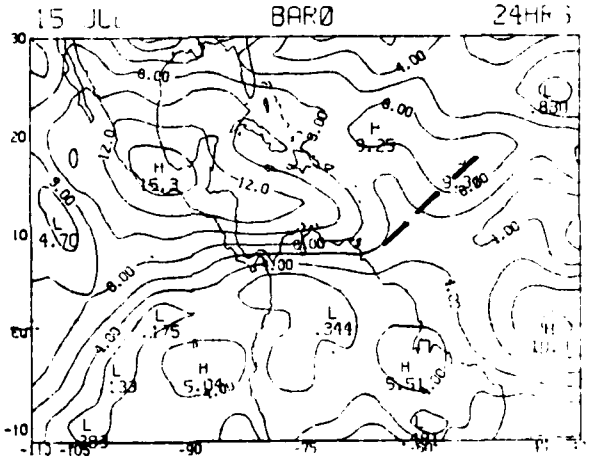

ISØTACHS

c

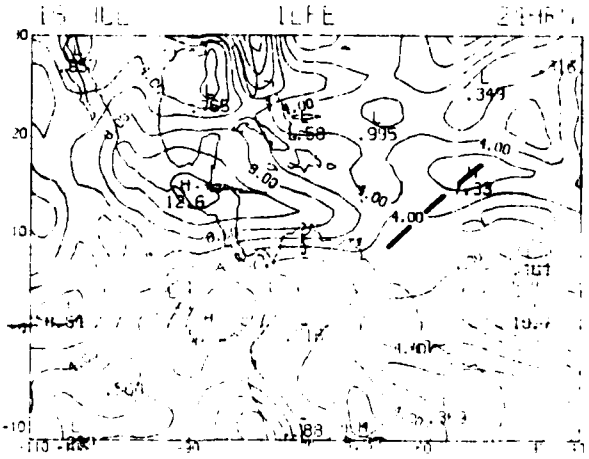

FIGURE 3.6 700 mb streamlines valid 16 July, 1200 GMT. (a) observation (b) barotropic (c) PE 24 hour forecast

a

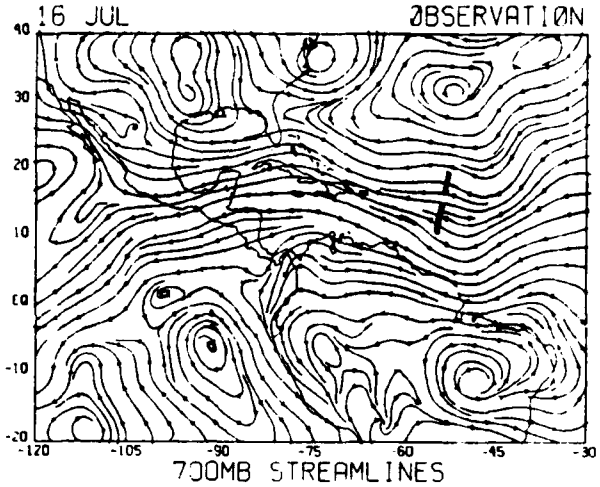
16 JUL
ØBSERVATIØN
40
30
20
10
0
-10
-20
-120
-105
-90
-75
-60
-45
-30
700MB STREAMLINES

b

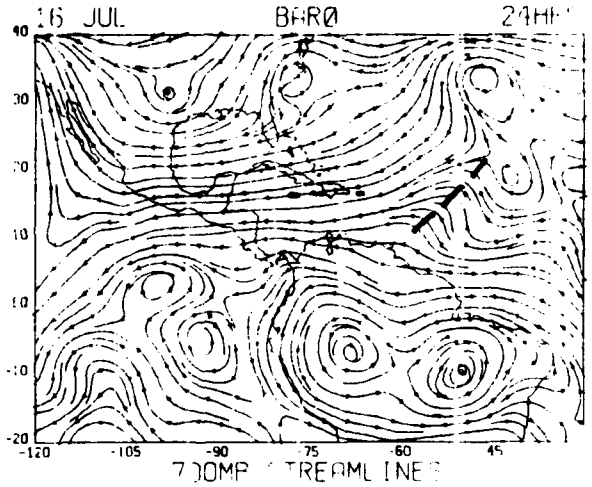
16 JUL
BARØ
40
30
10
-20
-120
-105
-90
-75
-60
45

c

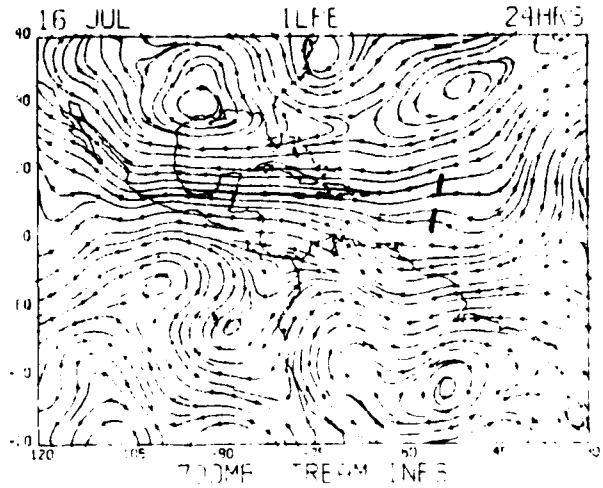
16 JUL
ILFE
40
0
-120
-90

FIGURE 3.7 700 mb streamlines valid 17 July, 1200 GMT. (a) observation (b) barotropic (c) PE 24 hour forecast

a

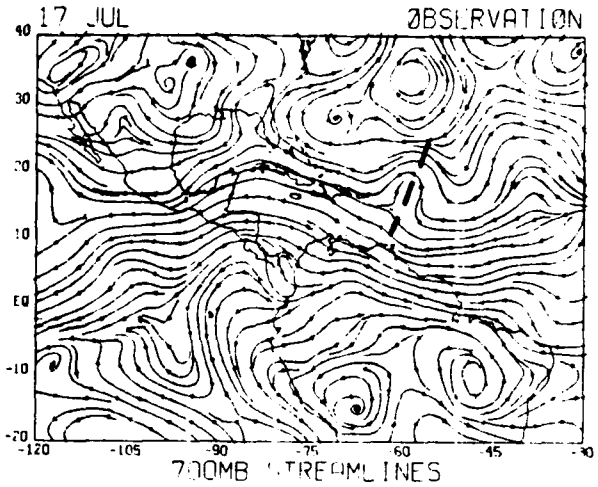
17 JUL
ØBSERVATIØN
40
30
20
10
EQ
-10
-20
-120
-105
-90
-75
-60
-45
-30
700MB STREAMLINES

b

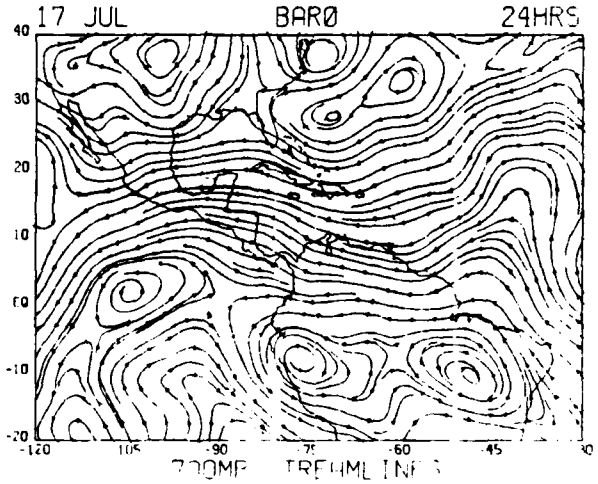
17 JUL
BARØ
24HRS
40
30
20
10
EQ
-10
-20
-120
-105
-90
-75
-60
-45
-30

c

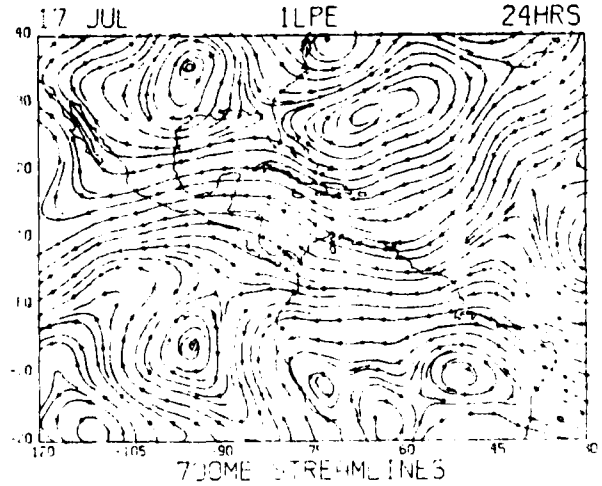
17 JUL
ILPE
24HRS
40
-120
-105
-90
-75
-60
-45
-30

different pattern (Fig. 3.8). Instead of becoming near-stationary, the wave continued moving steadily westward and strong upper level westerlies caused Claudette to weaken to a depression over Puerto Rico and eventually to a tropical wave over Hispaniola by 20 July. The opposite situation occurs after the morning of 20 July. The wave again started to develop and by late 21 July, Claudette had reformed as a tropical depression. Both models continued the movement quite well but ignored any development (Fig. 3.9).

Claudette continues as a tropical depression, moving gradually toward the Texas-Louisiana border. The barotropic 24 hour forecast valid 22 July does not show closed circulation, however the position is good (Fig. 3.10). The PE moves the wave too fast and south of the actual 22 July observation. In addition, an apparent weakening of the wave occurs towards the north. A difference in the forecast wind speeds is again seen between the barotropic and PE models, the PE model has underforecast the wind speeds by 2-4 mps (fig. 3.9).

The 24 hour forecast valid 23 July again shows both models weakening the system and trailing the actual position (Fig. 3.12). The PE model manages to forecast closed circulation, while the barotropic model continues to forecast an exaggerated wave. At this time, Claudette is coming in contact with a complicated system over the United States dominated by a large high pressure system. Once again, the PE model underforecasts the

FIGURE 3.8 700 mb streamlines valid 18 July, 1200 GMT. (a) observation (b) barotropic (c) PE 24 hour forecast

a

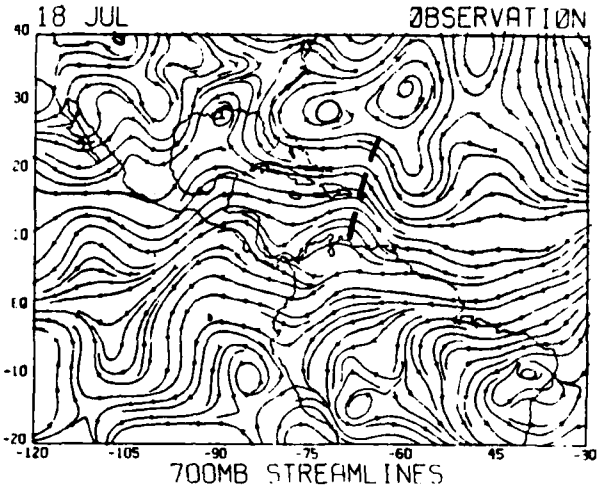
18 JUL
ØBSERVATIØN
700MB STREAMLINES

b

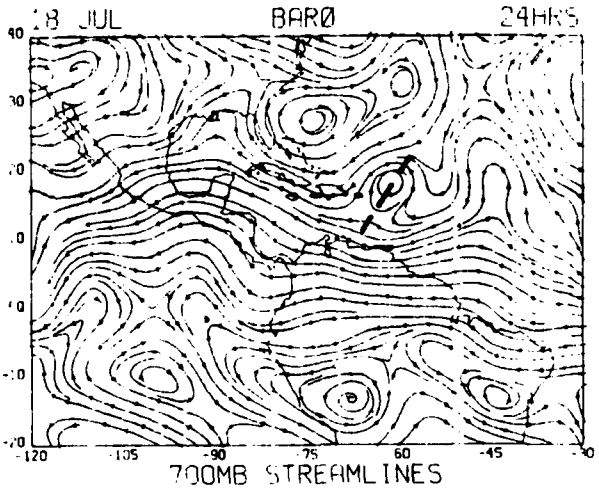
18 JUL
BARØ
24HRS
700MB STREAMLINES

c

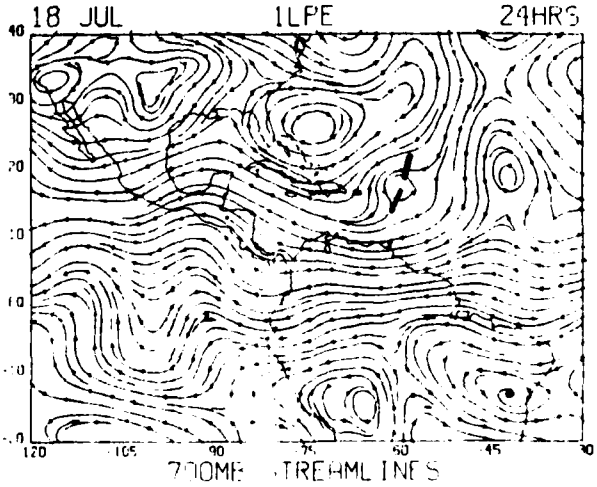
18 JUL
ILPE
24HRS

FIGURE 3.9 700 mb streamlines valid 21 July, 1200 GMT. (a) observation (b) barotropic (c) PE 24 hour forecast

a

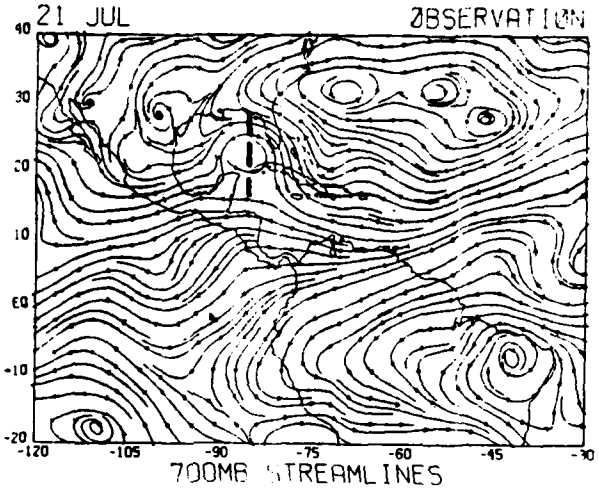
21 JUL
ØBSERVATIØN
40
30
20
10
EQ
-10
-20
-120
-105
-90
-75
-60
-45
-30
700MB STREAMLINES

b

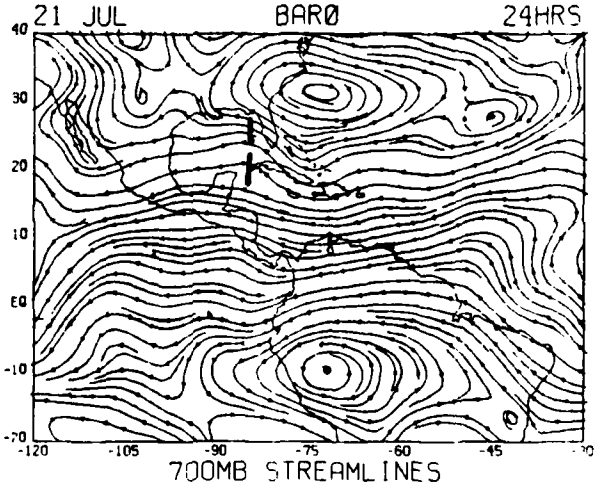
21 JUL
BARØ
24HRS
40
30
20
10
EQ
-10
-20
-120
-105
-90
-75
-60
-45
700MB STREAMLINES

c

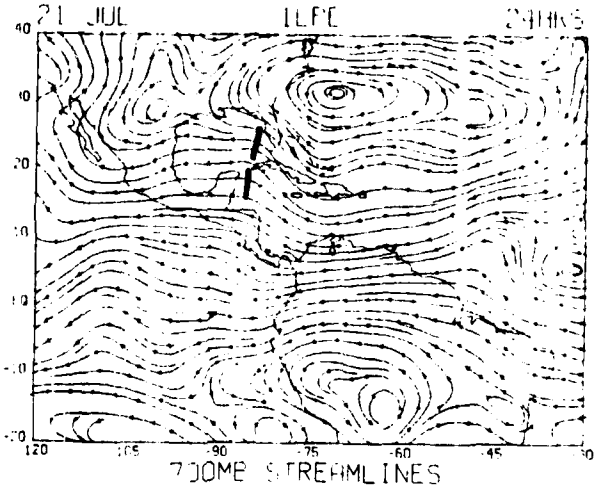
21 JUL
ILPE
40
20
-90
-75
-60
-45
700MB STREAMLINES

FIGURE 3.10 700 mb streamlines valid 22 July, 1200 GMT. (a) observation (b) barotropic (c) PE 24 hour forecast

a

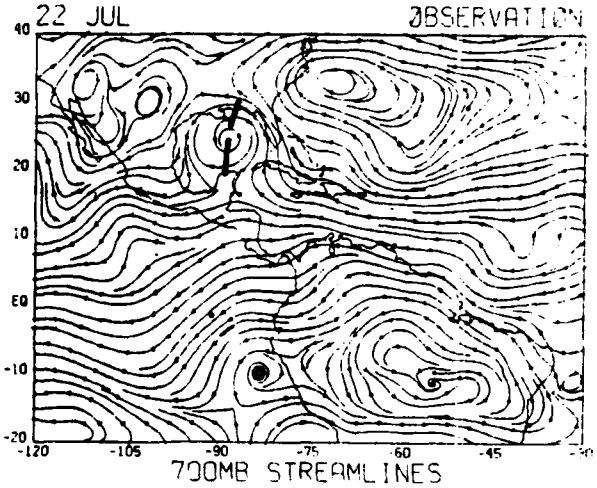
22 JUL
OBSERVATION
40
30
20
10
EQ
-10
-20
-120
-105
-90
-75
-60
-45
700MB STREAMLINES

b

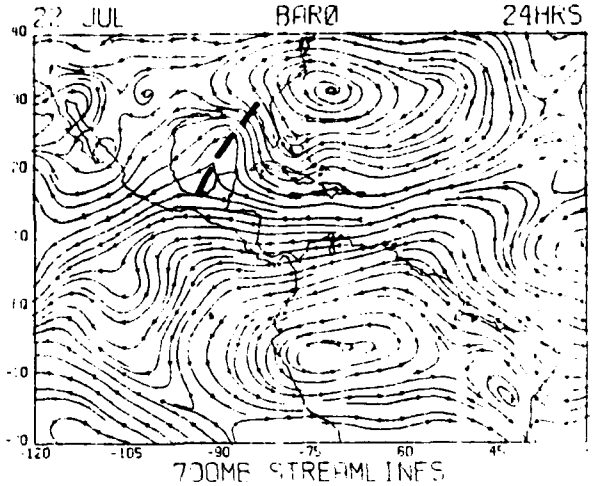
22 JUL
BARO
24HRS
40
-120
-105
-90
-75
-60
700MB STREAMLINES

c

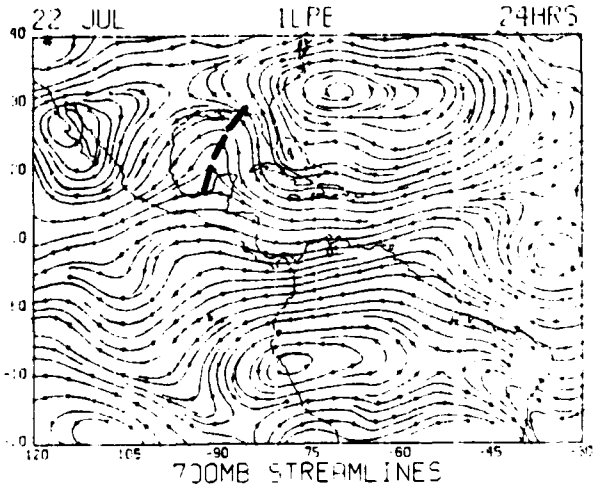
22 JUL
ILPE
24HRS
40
-120
-105
-90
-75
-60
-45
700MB STREAMLINES

FIGURE 3.11 700 mb isotachs valid 22 July, 1200 GMT.
(a) observation (b) barotropic (c) PE 24 hour forecast

a

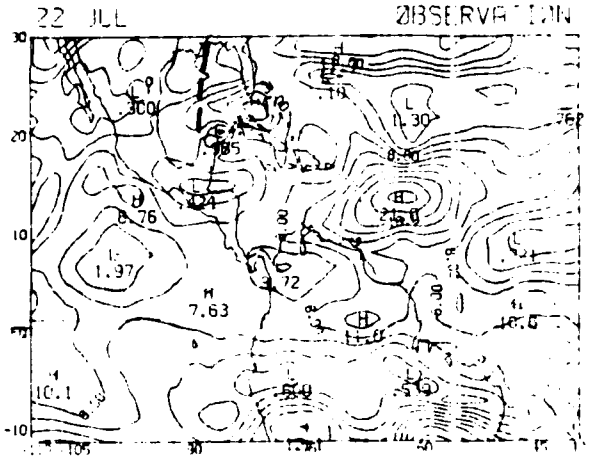
22 JUL
OBSERVATION

b

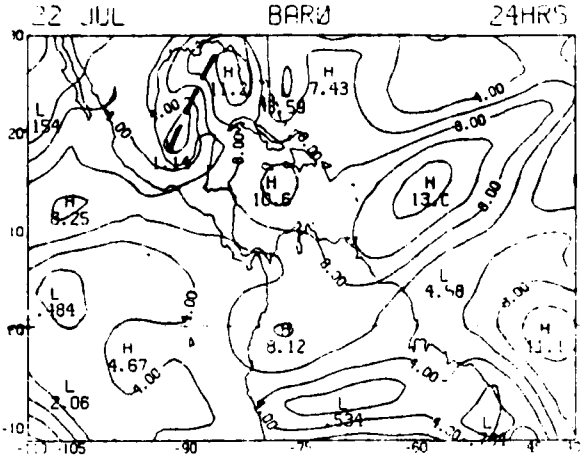
22 JUL
BARO
24HRS
ISOTACHS

c

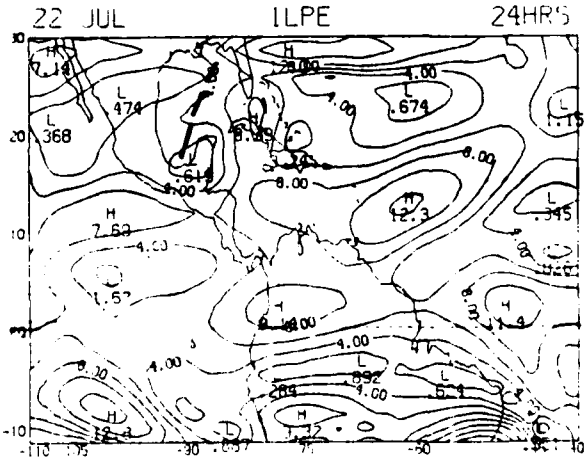
22 JUL
ILPE
24HRS
ISOTACHS

FIGURE 3.12 700 mb streamlines valid 23 July, 1200 GMT. (a) observations (b) barotropic (c) PE 24 hour forecast

a

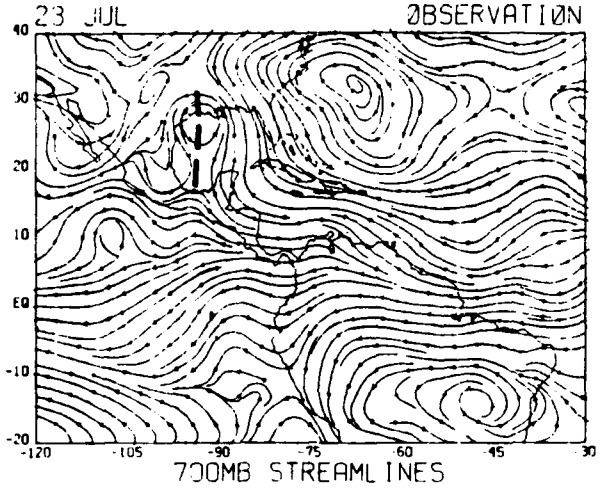
23 JUL
ØBSERVATIØN
40
30
20
10
EQ
-10
-20
-120
-105
-90
-75
-60
-45
-30
700MB STREAMLINES

b

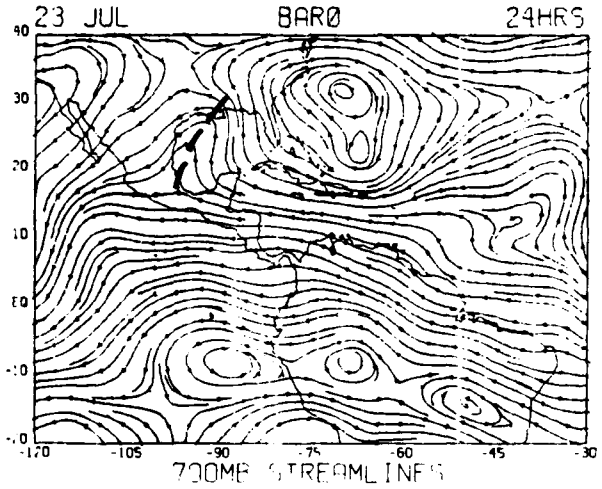
23 JUL
BARØ
24HRS
40
30
20
10
EQ
-120
-105
-90
-75
-60
-45
-30

c

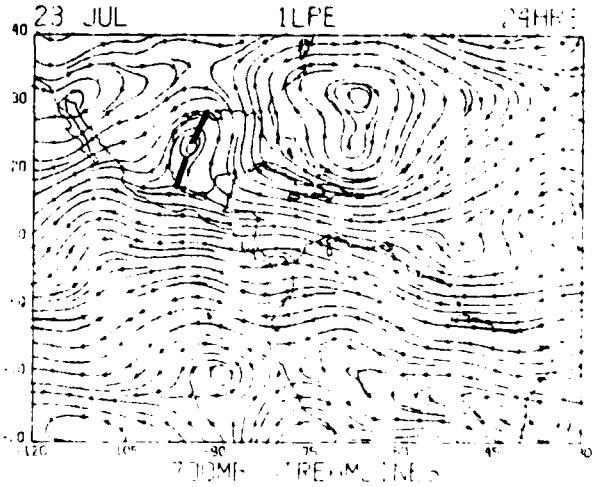
23 JUL
1LPE
40
30

winds by values ranging from 2-6 mps; actual values of 6-12 mps are noted with the largest errors occurring near the high (Fig. 3.13). In contrast, the barotropic model accurately forecast wind speeds with respect to the observed rotational winds of 4-10 mps, although still under forecasting with respect to the total wind speed.

From 24 July to 26 July Claudette made a tight loop and remained close to the coast. This allowed the system to remain close to the coast without weakening over land. The result was the record rainfall over Texas. Through this period, both the models correctly showed little movement, but repeatedly tried to weaken the circulation, convective processes being ignored by the models. Throughout this period, the PE model continually forecast weak wind speeds in the close vicinity of the large high pressure system, while the barotropic model performed better with respect to the wind speeds.

This short history of Claudette illustrates several weak forecasting situations. The most evident appear during periods of strengthening or weaking where important baroclinic effects, such as the upper level westerlies are very apparent. Also noted is the convective maintenance of Claudette over Texas and the effect of large, stationary systems near a weaker circulation or wave.

FIGURE 3.13 700 mb isotachs valid 23 July, 1200 GMT.
(a) observations (b) barotropic (c) PE 24 hour forecast

a

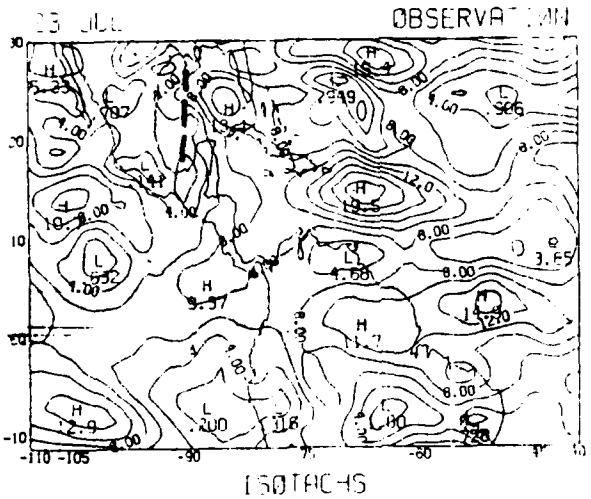
23 JUL
OBSERVATION
ISOTACHS

b

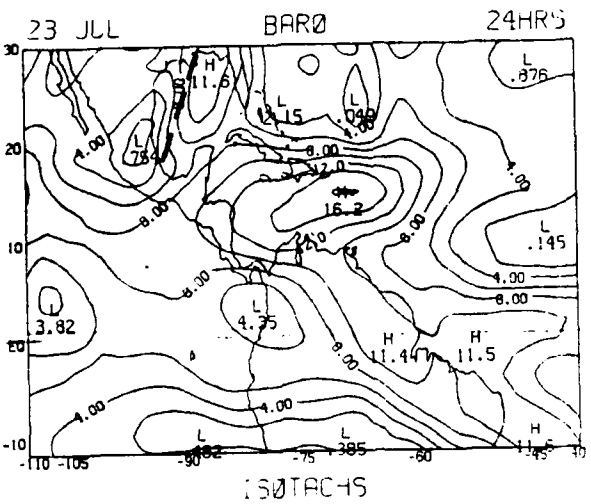
23 JUL
BARO
24HRS
ISOTACHS

c

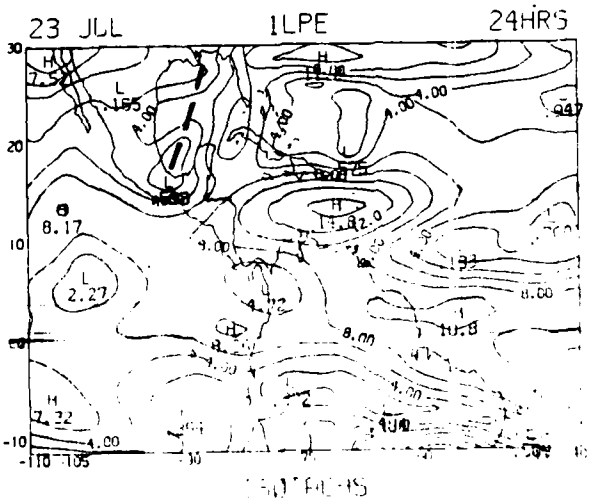
23 JUL
ILPE
24HRS

CHAPTER 4

Results of Prediction experiments Over the Atlantic Ocean and the Caribbean Sea

Ninety-three 96 hour experiments were carried out with the two single-level models, the barotropic and one-level PE. In addition to the inspection of specific forecast cases, two different verification scores have been computed as a general measure of the skill of the models. These are root mean square (RMS) errors for the vector, zonal and meridional winds, and the absolute correlation coefficient. A discussion of the verification system is included in the appendix.

The RMS vector deviation of the predicted winds relative to the verification winds is used as an estimate of the performace of the models. In addition, these RMS errors are compared to persistance, which is considered a relatively good forecasting tool in the tropics. The forecast area consisted of two rather different regions, accordingly the error statistics were calculated separately for each of the regions (Table 2). Region 1, the western region, included the Gulf of Mexico and Central America. It is an area of strong convective activity and

TABLE 2: Root mean square errors of forecast wind errors, valid 13 Aug. at 700 mb. Values are averaged over area and number of forecasts. Units are ms^{-1}

(i) Vector wind

	Region I		Region II	
	Forecast	Persistence	Forecast	Persistence
24 hour	3.30	2.83	3.15	3.89
48 hour	3.62	3.91	3.42	3.79
72 hour	3.56	4.47	3.68	5.60
96 hour	3.50	4.22	3.74	5.00

(ii) Zonal wind

	Region I		Region II	
	Forecast	Persistence	Forecast	Persistence
24 hour	2.03	1.97	2.44	2.94
48 hour	2.19	2.92	2.75	3.47
72 hour	2.28	3.34	2.83	4.35
96 hour	2.34	2.94	2.90	3.97

(iii) Meridional wind

	Region I		Region II	
	Forecast	Persistence	Forecast	Persistence
24 hour	2.20	2.40	1.99	2.55
48 hour	2.88	2.60	2.04	3.30
72 hour	2.73	2.97	2.35	3.53
96 hour	2.61	2.02	2.36	3.05

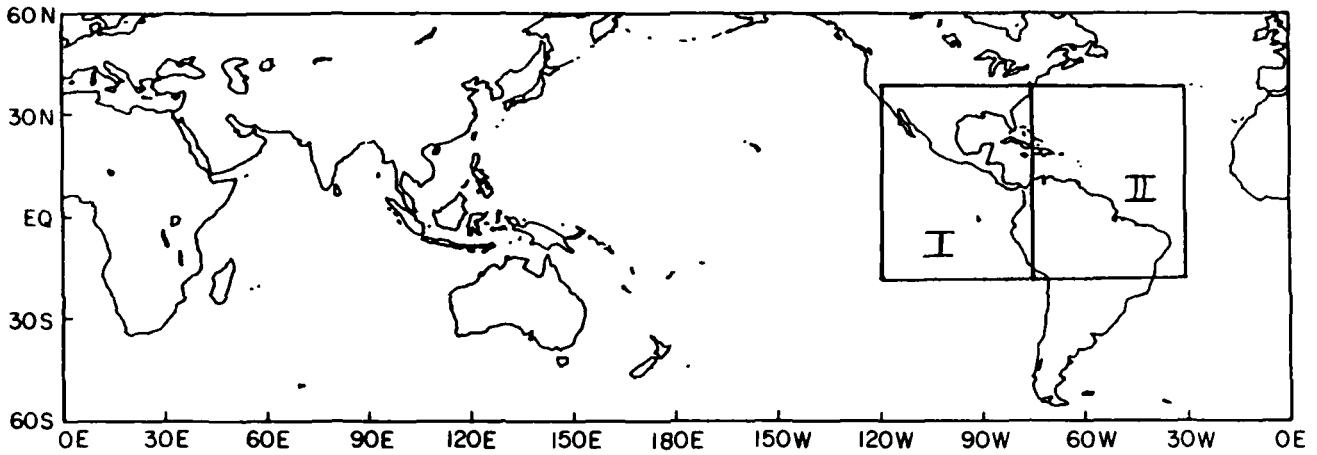

FIGURE 4.1 Domain of numerical forecasts. Region I comprises an area of 120°W-75°W, 20.625°S-29.375°N and Region II an area of 75°W-30°W, 20.625°S-29.375°N

persistant divergent flow. Region 2 is the eastern region which covers much of the tropical Atlantic Ocean (Fig. 4.1).

The root mean square average errors for the forecasts in Regions 1 and 2 are presented in Table 3a and 3b.

4.1 Verification - Region 1.

Region 1 shows rather poor performance by both models. The barotropic forecast results in errors which exceed those of persistence at all forecast periods, while the one-level PE model barely exceeds persistence at only the 24 hour period. In addition, it is noted that the errors from the nondivergent model forecast values at 24 hours that are only slightly worse than those of the divergent model. The short term performance of the barotropic model at times outperformed the one-level PE, especially with regards to the wind speeds. The size of the RMS errors varied much more with the barotropic model than with the one-level PE, and when the barotropic model did outperform the one-level PE at 24 hours, the margin was generally not large.

4.2 Verification - Region 2.

Region 2 presents slightly different results. The barotropic model again has poor results, failing to match persistence at any forecast period. However, the one-level PE RMS errors beat

TABLE 3A: Root mean square error of forecast wind errors at 700 mb for Region I. Values are averaged over area and number of forecasts. Units are ms^{-1}

(i) Vector wind

	Barotropic Model	One-level PE Model	Persistence
24 hour	3.17	3.01	3.07
48 hour	4.82	4.13	4.08
72 hour	5.24	4.58	4.41
96 hour	5.39	4.80	4.43

(ii) Zonal wind

	Barotropic Model	One-level PE Model	Persistence
24 hour	2.22	2.12	2.11
48 hour	3.57	3.05	2.93
72 hour	4.01	3.44	3.29
96 hour	4.07	3.65	3.35

(iii) Meridional wind

	Barotropic Model	One-level PE Model	Persistence
24 hour	2.23	2.12	2.22
48 hour	3.20	2.76	2.82
72 hour	3.31	2.99	2.91
96 hour	3.47	3.10	2.87

TABLE 3B: Same as Table 3a except for Region II

(i) Vector wind

	Barotropic Model	One-level PE Model	Persistence
24 hour	3.78	3.31	3.48
48 hour	5.29	4.29	4.64
72 hour	5.49	4.67	4.93
96 hour	5.54	4.75	4.82

(ii) Zonal wind

	Barotropic Model	One-level PE Model	Persistence
24 hour	2.69	2.37	2.38
48 hour	4.04	3.13	3.32
72 hour	4.28	3.56	3.68
96 hour	4.36	3.76	3.73

(iii) Meridional wind

	Barotropic Model	One-level PE Model	Persistence
24 hour	2.63	2.29	2.52
48 hour	3.34	2.91	3.20
72 hour	3.38	2.99	3.22
96 hour	3.36	2.86	3.01

persistence through 96 hours. The divergence contained within the PE model would seem to be a more important component in the average weather regime than it is in the western region. Inspection of the absolute correlation coefficients show the barotropic and one-level PE forecasts both showing skill during the first 24 hours, with results becoming poor by 48 hours. (Table 3c)

4.3 Flow field

The poor performance of the barotropic model past 24 hours and of the one-level PE model past 48 hours can be noted via the average absolute correlation coefficients. Visual inspection of the flow fields would seem to bear this out, (Fig. 4.2 a through m). The small scale perturbations are carried through the 48 hour forecast as generally recognizable features. The predicted intensities of these features, whether of wind speeds or the amplitude of the wave itself, quickly become quite different from the observed after 24 hours. As seen earlier, the models have obvious errors within 24 hours whenever development or decay is occurring. This is most recognizable in the amplitudes of the features and to a lesser extent in the phase speeds, although both are apparent.

Past 48 hours, large features such as high or low pressure systems remain identifiable, although the barotropic model begins to smooth the flow field. Poor positioning of quasi-stationary

TABLE 3C: Absolute correlation coefficients between forecast and observed winds at 700 mb for Region I. Values are averaged over number of forecasts.

	Barotropic Model	One-level PE Model	Persistence
24 hour	.67	.68	.67
48 hour	.39	.48	.46
72 hour	.32	.39	.39
96 hour	.29	.34	.40

Absolute correlation coefficients between forecast and observed winds at 700 mb for Region II. Values are averaged over a number of forecasts.

	Barotropic Model	One-level PE Model	Persistence
24 hour	.64	.68	.66
48 hour	.40	.47	.47
72 hour	.35	.39	.42
96 hour	.35	.36	.43

a

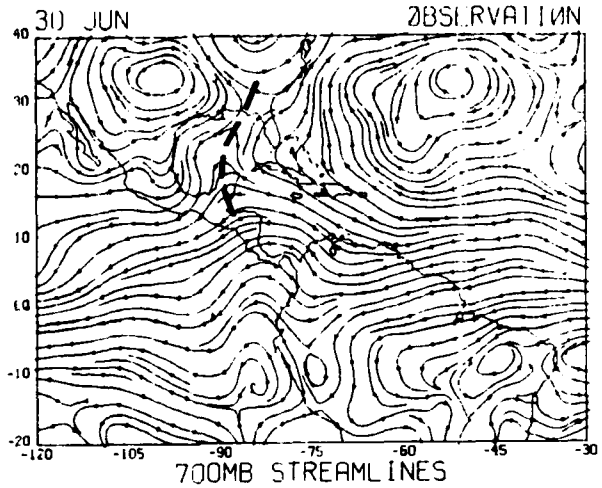

FIGURE 4.2 (a) to (m) refers to streamline analysis characteristics which often lead to good forecasts (a) is the observation for 30 June, 1979 at 1200 GMT. (b), (c) and (d) are the 24 hour observation and the barotropic and one-level PE predictions respectively. (e), (f), (g); (h), (i), (j); and (k), (l), (m) are the same as (b), (c), (d) but for the 48, 72, and 96 hours respectively.

b

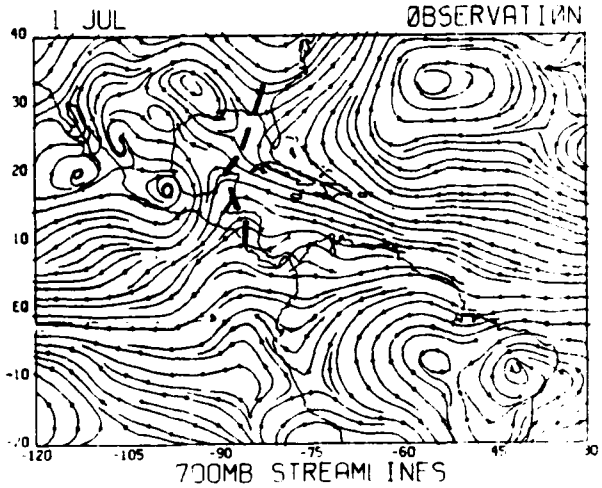
1 JUL
ØBSERVATIØN
40
30
20
10
EQ
-10
-20
-120
-105
-90
-75
-60
45
30
700MB STREAMLINES

c

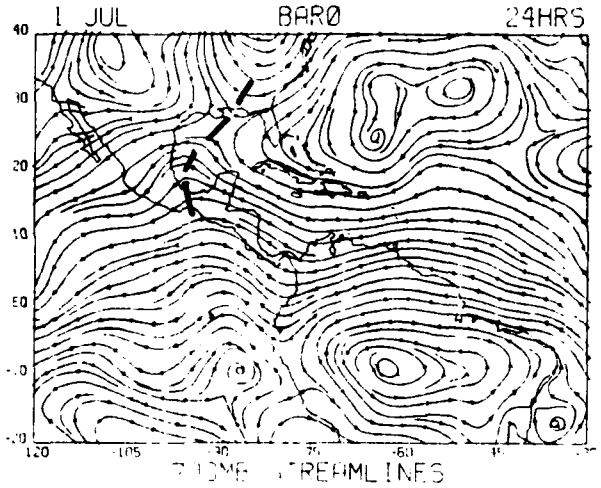
1 JUL
BARØ
24HRS
40
30
20
10
EQ
-10
-20
-120
-105
-90
-75
-60
45
30
700MB STREAMLINES

d

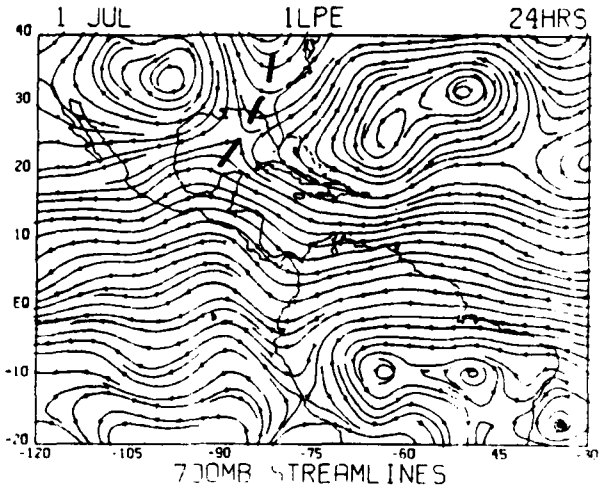
1 JUL
ILPE
24HRS
40
30
20
10
EQ
-10
-20
-120
-105
-90
-75
-60
45
30
700MB STREAMLINES

e

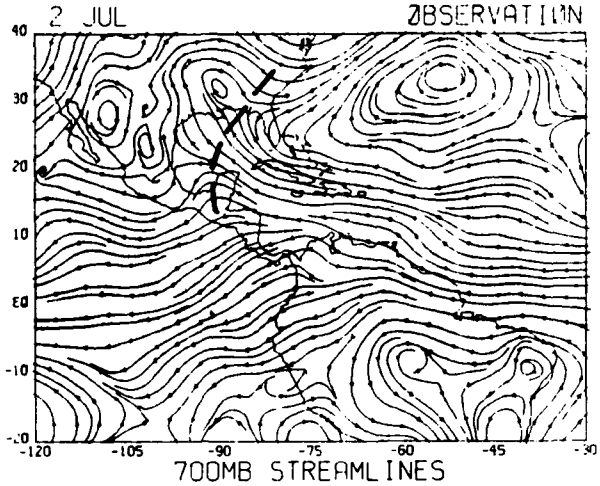
2 JUL
ØBSERVATIØN
700MB STREAMLINES

f

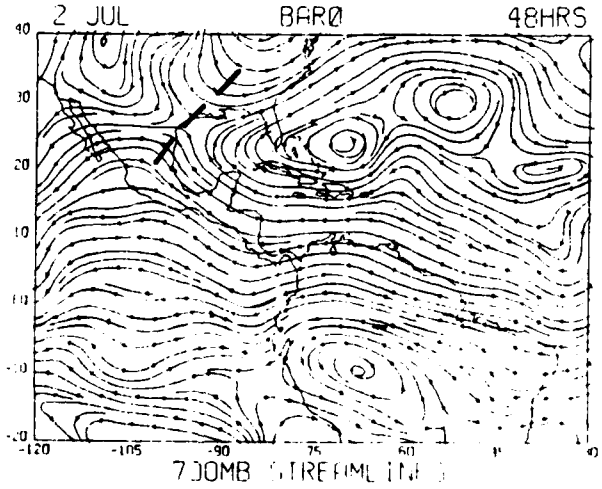
2 JUL
BARØ
48HRS

g

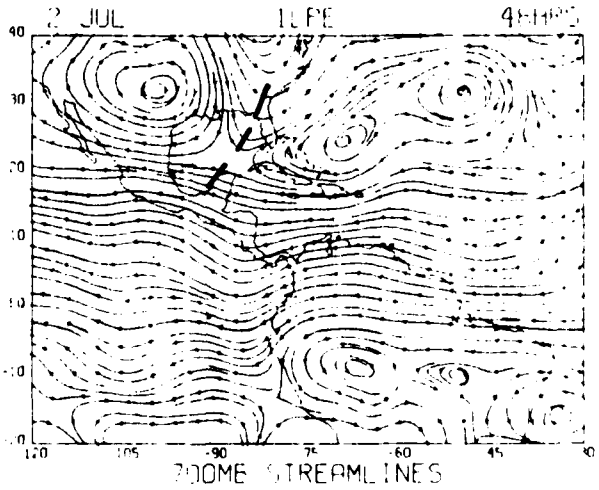
2 JUL
700MB STREAMLINES

h

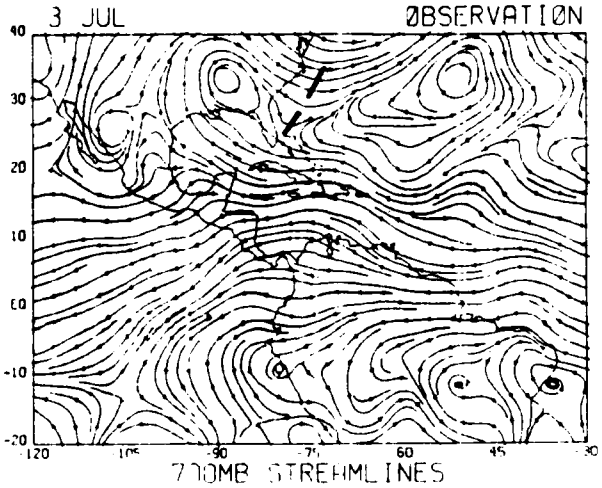
3 JUL
ØBSERVATIØN
40
30
20
10
0
-10
-20
-120
-105
-90
-75
-60
-45
-30
700MB STREAMLINES

i

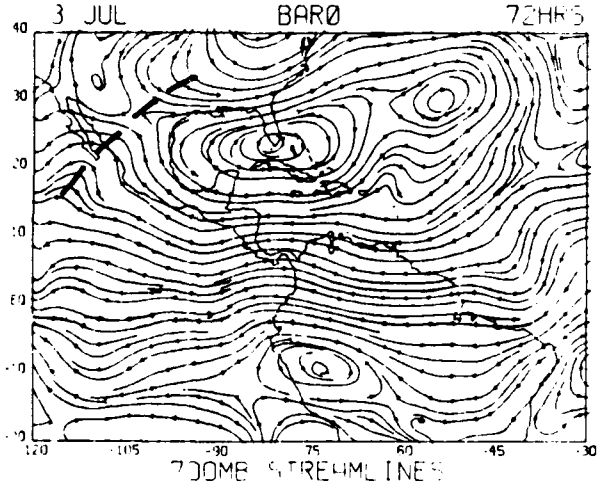
3 JUL
BARØ
72HRS
40
30
20
10
0
-10
-20
-120
-105
-90
-75
-60
-45
-30
700MB STREAMLINES

j

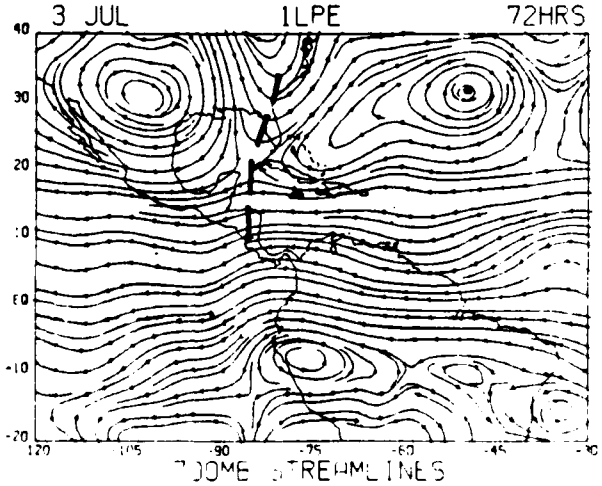
3 JUL
ILPE
72HRS
40
30
20
10
0
-10
-20
-120
-105
-90
-75
-60
-45
-30
700MB STREAMLINES

k

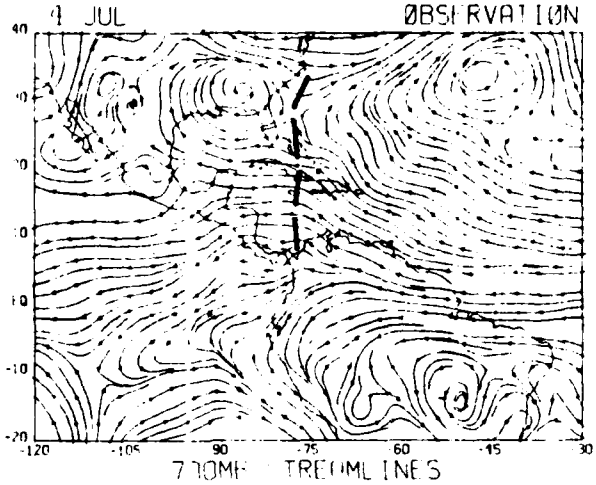

l

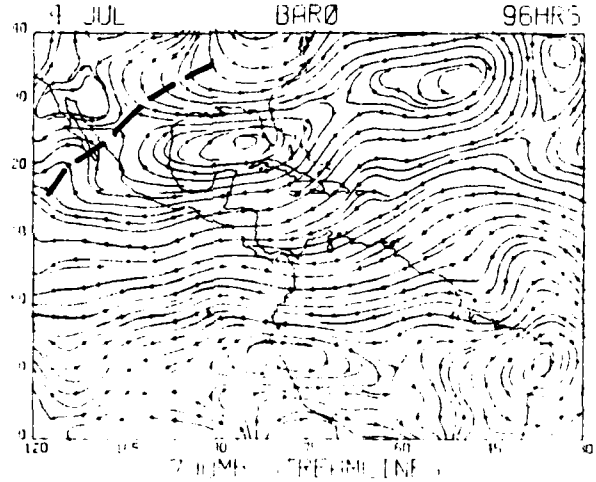

m

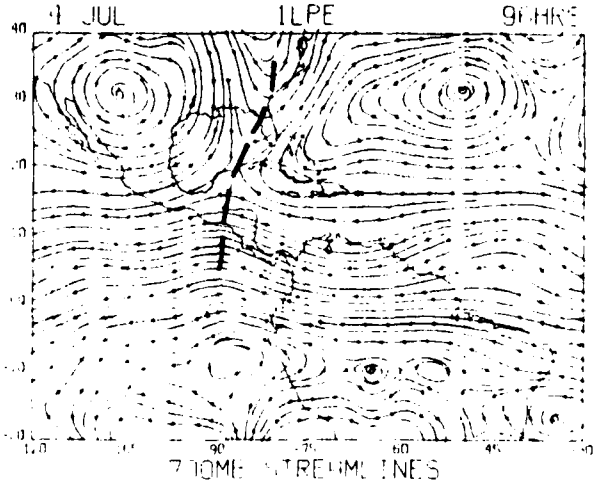

systems often occurs, such as the Bermuda High and the highs over South America. The various closed circulations remain only as ridges and troughs, while false closed circulations may appear. Inspection of the two model's forecasts past 48 hours suggests that the better statistical results of the PE arise from a better description of the wind fields; the positioning of the major systems appear to err by equal amounts.

The barotropic forecast at 72 hours loses representation of even the largest features. An example is of the high pressure system over South America which often is forecast as zonal flow. The same situation occurs to the one-level PE model, although to a lesser degree as representations of large troughs are often depicted through the 72 hour forecast.

By the 96 hour forecast, both models often forecast synoptic scale circulations which are severely displaced by a distance as great or greater than the systems themselves. The result, of course, would be a forecast of a high pressure system where a low actually occurs.

4.4 Representative Weather Regimes

A discussion of a good and poor forecast follows. These examples have been chosen as representative examples of recognizable weather regimes which consistently produced good or poor results. Some of the qualities of a good forecast included a

large amount of zonal flow, with disturbances embedded in that flow being of only minor size. For a good forecast large permanent type systems should not be a large part of the region. They are usually confined to the northen or southern boundaries, (Fig. 4.2a). Such systems which are usually present are the large subtropical high off the east coast of the United States and also over the South American continent. On a smaller scale, closed circulations are usually only of relatively small size. Although the predicted wind speeds of these systems are usually too low, their areal coverage is small and they have little effect on the statistical region. Two distinct differences appear repeatedly when good forecast and poor forecast series are compared. First, the large, northern semipermanent high extends further southward and into the zonal flow, (Fig. 4.3). The forecasts will move this system along with the zonal flow while it actually verifies as virtually permanent. Position errors of the center of these highs are as large as 15°. Another large source of error which occurs quite frequently are apparent divergent circulations which develop in the western Caribbean, across Central America and especially just off-shore west of Central America. Notable in these instances is the very different analysis of the observed data resulting from the barotropic and one-level models. The implication is of large amounts of convective circulation which is accounted for by neither model's forecast.

a

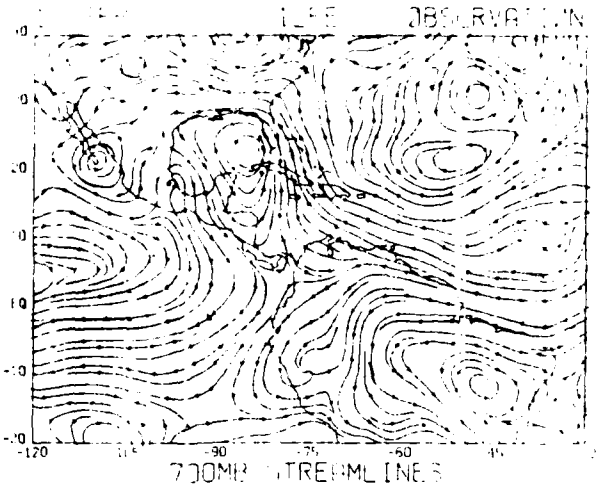

b

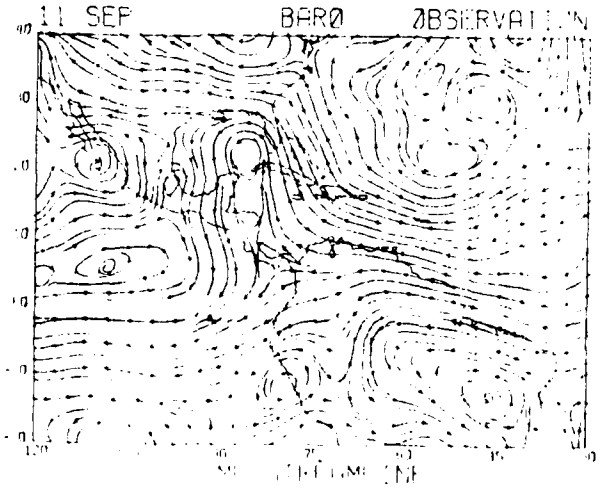

FIGURE 4.3 Streamline analysis showing typical characteristics which often lead to poor forecasts (a) observed rotational winds (b) observed total winds (rotational and divergent)

CHAPTER 5

A Review of Past Studies

The barotropic and one-level primitive equation models have previously been tested over three rather diverse regions, (Fig. 5). Adejokun and Krishnamurti (1982) studied a large area centered over the Atlantic and West Africa. A region including the Indian Ocean, Indonesia and the western Pacific Ocean was studied by Yap et al. (1983) during the northern winter. This study will be referred to as the winter monsoon. Atma et al. (1984) looked at a similiar region during the northern summer and this region will be referred to as the summer monsoon. The Adejokun results over Africa and the Atlantic Ocean are by far the best. This is an encouraging aspect for the western Atlantic due to the large number of African waves which cross the Atlantic, and particularly since approximately half of the tropical cyclones of the Atlantic Ocean originate from intensifying African waves. The results from the studies of the winter and summer monsoons differ widely, not only between the different topographical areas, but they also are dependent on the time of the year. The results are generally poor and the performance of the models should be considered in light of the important physical processes

FIGURE 5. Domain of numerical forecasts. Areas are as in Table 4. (a) Regions III, IV and V, (b) Regions VI and VII

a

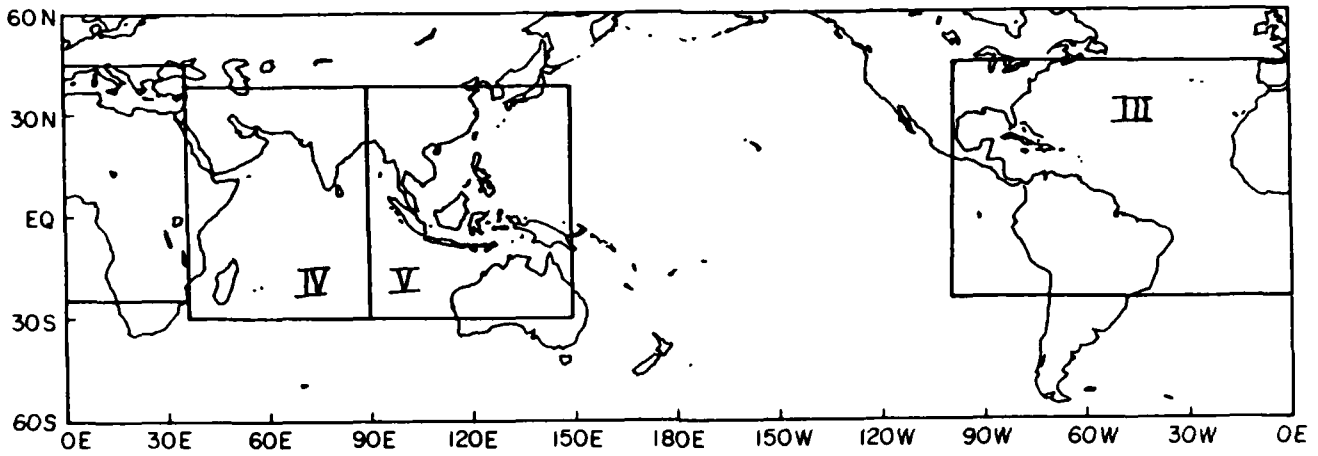
60N
30N
EQ
30S
60S
0E
30E
60E
90E
120E
150E
180E
150W
120W
90W
60W
30W
0E
III
IV
V

b

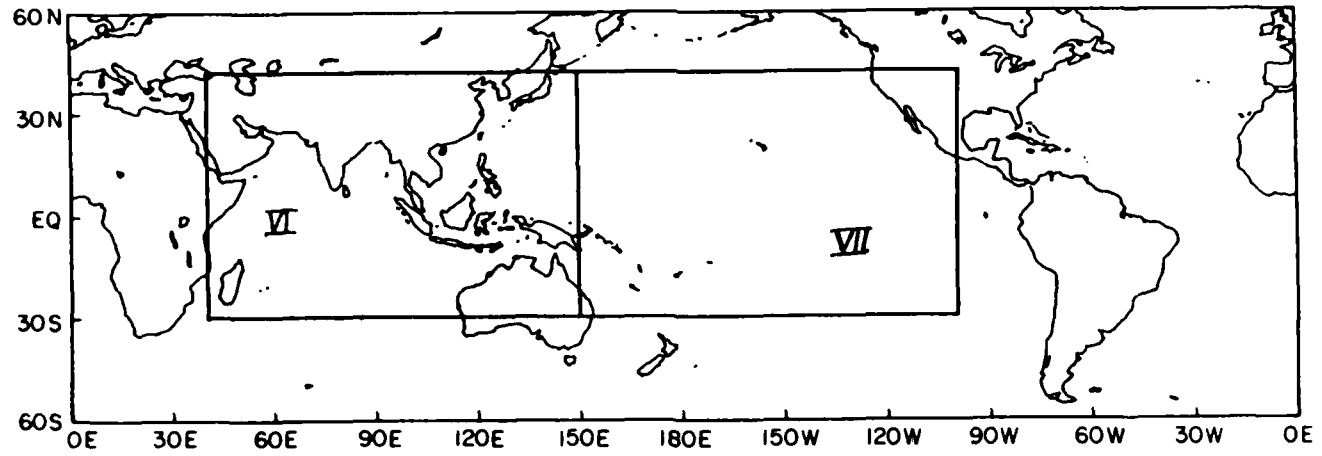
60N
30N
EQ
30S
60S
0E
30E
60E
90E
120E
150E
180E
150W
120W
90W
60W
30W
0E
VI
VII

which dominate these regions, such as strong convective and divergent circulations.

5.1 The Atlantic and Western Africa

The Adejokun experiment consisted of 52 forecasts for June to September 1979. He found the flow field to be in generally good agreement with respect to the main synoptic features up to 72 hours. However, beyond 72 hours, the positions of some features seem to depart significantly from the observed. Both models advected the tropical waves fairly accurately for the first 48 hours, a predicted trough position within 1-2° latitude of the observed. Beyond the 48 hour period, the phase speed of both models deteriorated. The average phase speeds of the barotropic and PE model were, respectively, 5.4 deg/day (6.9 mps) and 6.7 deg/day (8.6 mps). This is compared to an observed phase speed of 6.2 deg/day (8.0 mps). Both models showed a decrease in the maximum wind speeds in the easterlies. This was traced to the boundary conditions of u, v and z being set to zero, resulting in inadequate middle-latitude interaction. In addition, main differences in the flow field occurred at the north and south boundaries. In general, the models increased the wind speed in low speed areas and decreased the speed in high speed areas.

5.2 The Summer Monsoon

The forecasts over the Indian Ocean and Indonesia, the summer monsoon region, were for a period from 1 June to 31 July, 1979. The first 10 days of the period show good results, a period before either the westerly monsoon over India or the easterly monsoon over Indonesia has shown any strong activity. Afterwards, both monsoons begin activity which lasts through the summer season. During this early 10-day period both models show good positioning of troughs and ridges, especially during the first 24 hours. The one-level PE performs better, with reasonable results up to 48 hours. In addition, the PE model shows better results over the mountainous regions due to the inclusion of terrain heights. Once the monsoon season begins, the models fare poorly, the tropical easterly jet and the strong Hadley overturning are persistent features which dominate the region.

5.3 The Winter monsoon

The final study is again over the Indian Ocean-western Pacific, but for the period of 1 December 1978 to 19 January 1979 during the winter monsoon. Here, the subtropical high belts are simulated reasonably well during the first 48 hours. Clearly shown was the good agreement between the observed and forecast positions of the tropical waves over the Central Pacific Ocean. The story is different over the western region. This western

region has strong meridional overturning of the Hadley cell. In this region large quasi-stationary features remain present, a mechanism for which is lacking in the models. A large proportion of the forecast errors are credited to these large systems. Flow over the mountainous regions remains difficult to simulate and terrain in the PE model sometimes leads to areas of excessive winds. Still, the PE streamlines look more realistic in these areas compared to the barotropic model. The errors in this western region were slightly larger from the divergent model than from the non-divergent model. The divergence within the PE model doesn't describe the overturning/Hadley type circulation. The absence of divergence in the barotropic model leads to better performance in the western region. In the east, over the central Pacific, the model's error statistics were better than the western region, however, rather poor quality when compared to west Africa and the Atlantic Ocean. This can be explained in part by the differences in the two types of waves found in the respective regions. Over the Atlantic, the African waves have their maximum amplitude around 700 mb and have been shown to draw energy from the low level west African easterly jet (Burpee, 1972). No comparable level wind current exists near the middle troposphere over the western Pacific during the northern winter season. Instead, the easterly waves in this region have their largest amplitude closer to the 800 mb surface and are influenced more by the boundary layer dynamics and the related divergence.

The largest amplitude of the African waves are well separated from the boundary layer and are located near the level of non-divergence. Better results may be achieved in this area with a forecast carried out at a lower pressure level.

The vector root mean square error of the forecast and the error of persistence are compared for each of the above regions in Table 4.

TABLE 4: Root mean square errors of forecast wind errors. Regions I and II were discussed in Chapter 4 and are included for comparison. Domains are shown in Figs. 4.1 and 5.

Region	Domain/ Period	Forecast Hour	Barotropic Model	One Level PE Model	Persistence
I Central America	120°W-75°W 20.625°S-29.375°N 15 June - 15 Sept 1979	24	3.16	3.01	3.07
		48	4.82	4.12	4.08
		72	5.24	4.57	4.41
		96	5.38	4.80	4.43
II Western Atlantic South America	75°W-30°W 20.265°S-39.375°N 15 June - 15 Sept 1979	24	3.78	3.31	3.48
		48	5.20	4.29	4.64
		72	5.48	4.67	4.92
		96	5.53	4.74	4.82
III West African Monsoon	100°W-38°E 25°S-45°N 16 June - 15 Sept 1979	24	4.82	4.97	5.47
		48	6.15	6.02	6.50
		72	6.87	6.31	6.49
		96	7.09	6.44	6.66
IV Indian Summer Monsoon	30°E-90°E 30°S-39.375°N 1 June - 31 July 1979	24	5.13	4.84	4.09
		48	7.15	6.10	5.43
		72	8.64	6.97	6.05
		96	9.30	7.79	6.34
VI Summer Monsoon Over South-east Asia	90°E-150°E 30°S-39.375°N 1 June - 31 July 1979	24	4.51	4.53	4.25
		48	6.61	5.97	5.76
		72	7.30	6.86	6.48
		96	7.52	7.35	6.72
VI Winter Monsoon	41.25°E-150°E 30°S-45°N 1st Dec 1978 19th Jan 1979	24	4.9	5.3	4.9
		48	6.0	6.4	5.9
		72	7.0	7.4	6.4
		96	7.7	8.1	6.6
VII Central Pacific Ocean Domain Northern Winter	150°E-101.25W 30°S-45°N 1st Dec 1978 19th Jan 1979	24	6.6	6.2	6.4
		48	8.9	8.2	8.4
		72	9.8	9.4	9.2
		96	10.1	9.8	9.6

CHAPTER 6

Summary and Conclusions

Ninety-three prediction experiments have been carried out in this study as well as a review of past experiments, resulting in a total of approximately 980 regional experiments made with two single level models. The simple barotropic model does not have much skill over most of the tropics except for the West African monsoon region (domain 3), which also includes the Eastern Atlantic Ocean. In this region this simple model has a skill beyond that of persistence for about 2 days. Over most regions the skill is less than 24 hours. Over West Africa the low level easterly jet around 600 mb is known to be barotropically unstable (Rennick, 1976). The African waves over this region receive energy from the local zonal flows as they propagate westward (Tripoli and Krishnamurti, 1975). Beyond 48 hours, the deterioration of the barotropic forecast over this region is attributed to a collapse of the basic zonal easterlies and the west African monsoon. Adiabatic models cannot sustain a source of energy for the African monsoons on a time frame beyond 2 days (Krishnamurti *et al.*, 1979).

The failure of the simple barotropic model over most regions is due to the crucial role of convection and associated divergent motions. The lowest skill of the model was noted over the winter monsoon regions where the diabatic processes and divergent circulations are dominant.

The single level primitive equation model performs better than the simple vorticity conserving model in all regions except the winter monsoon (domain 6), where extremely strong divergent circulation exists. Still, useful skill is exhibited only over the following regions:

Region I	Central America during northern summer to 1 day
Region II	Western Atlantic and South America during northern summer to 4 days
Region III	West African monsoon and Eastern Atlantic during northern summer to 4 days
Region VII	Central Pacific Ocean during northern winter to 1 day

The results over West Africa, the Atlantic Ocean and South America do seem to suggest the practical utility of the single level primitive equation model in specific areas of the tropics. However, the performance over the Asian monsoon regions is generally quite poor, where the role of diabatic heating and divergent motions are dominant. In addition, the experiments over the Atlantic and Central America (domains 1 and 2) related problems the single level PE model encountered near the location

of large quasi-stationary systems. Large underforecasting of wind speeds by the single-level PE model near these systems often lead to better short-term performance of the non-divergent model.

The single level PE model also displayed strong tendencies to significantly reduce the strength of smaller closed circulations such as tropical depressions. Hence, the convective-driven circulations would be eliminated from the forecasts after 48 hours. Further improvements in such areas as this may be possible with the parameterization of a cumulus mass flux in the vorticity and the momentum equations, Cho, et al.(1983). This requires an additional equation for the prediction of the mass flux. According to this study, the budget of convective tropical disturbances can be better represented by the parameterization of the cumulus transport of vorticity. Addition of this parameterization would consist of a relatively simple modification of the system of equations of the single level primitive equation model. Significant results would further increase the attractiveness and usefulness of a model which can be run operationally on fairly small computers.

APPENDIX

A.1 Verification System

The verification scores used in this study essentially follow those suggested by the WMO/CAS Working Group on Weather Prediction Reserach (1978) and used at the ECMWF (Hollingsworth et al., 1980; Nieminen, 1983). They are

(a) root mean square error for forecasts and persistence

(b) standard deviation of error for forecast and persistence

and (c) absolute correlation, which is the correlation between predicted and the verifying fields.

Following Nieminen (1983), the following symbols stand for:

A_v = verifying field

F = forecast

g_i = weight for each grid point in the verification area

g_T = total weight in the verification are

$(\bar{\ })$ = area mean

the verification scores may be written as area means,

$$\text{area mean, } \bar{A} = \frac{\Sigma A_i g_i}{g_T},$$

where the weight g_i is the cosine of the latitude. This accounts for the decreasing grid interval along latitudes in the meridional direction.

$$\text{RMS error} = \sqrt{\frac{\Sigma(F-A_v)^2\, g_i}{g_T}},$$

$$\text{standard derivation of error} = \sqrt{\frac{\Sigma\left[(F-A_v)^2 - (\overline{F-A_v})\right]^2 g_i}{g_T}},$$

$$\text{absolute correlation} = \frac{\Sigma\left[(F-\overline{F})\ (A_v-\overline{A_v})\right]g_i}{\sqrt{\Sigma(F-F)^2 g_i\ \Sigma(A_v-A_v)^2 g_i}}.$$

Since verification in this study deals mainly with vector winds, the results of the individual wind components were combined, i.e.,

$$\text{RMS (V)} = \sqrt{\left[\text{RMS(u)}\right]^2 + \left[\text{RMS(v)}\right]^2}$$

$$\text{STD (V)} = \sqrt{\left[\text{STD(u)}\right]^2 + \left[\text{STD(v)}\right]^2}$$

$$\text{correlation, R(v)} \approx \sqrt{1/2\ \left[\text{R(u)}^2 + \text{R(v)}^2\right]}$$

A.2 Verification area

Due to the boundary effects, the verification of the forecast fields is carried out over a smaller inner domain (5 grid points are eliminated along the boundaries) and calculated separately for each of the regions.

REFERENCES

Adejokun, J.A. and T.N. Krishnamurti, 1983: Further numerical experiments on tropical waves. TELLUS, 35A, 398-416.

Arakawa, A., 1966: Computational design for longterm numerical integration of the equations of atmospheric motions. J.Comp. Phys., I, 119-143.

Atma, K., A. Kumar, T.N. Krishnamurti, 1984: Numerical weather prediction experiments over the monsoon region. FSU Report, Tallahassee, Florida 32306, USA.

Burpee, R.W., 1972: The origin and structure of easterly waves on the lower troposphere of north Africa. Journ. Atm. Sci., 29, 77-90.

Cho, H.R., M.A. Jenkins and J. Boyd, 1983: A first order vorticity equation for tropical easterly waves. J. Atmos. Sci., 40, 958-968.

Gates, W.L. and A.B. Nelson, 1975: A new (revised) tabulation of Scripps Topography on a 1° global grid. Part 1: Terrain heights. Rept. No. R-1276-1-ARPA, Rand Corporation. Santa Monica, California.

Haltiner, G.J., and R.T. Williams, 1980: Numerical Prediction and Dynamic Meteorology. John Wiley and Sons, Inc., 477 pp.

Hebert, P.J., 1980: Atlantic hurricane season of 1979. Mon. Wea. Rev., 108, 973-990.

Julian, P.R., 1981: An evaluation of the FGGE tropical observing system. Presented at International Conference on Preliminary FGGE Data Analysis and Results, Bergen, Norway.

Krishnamurti, T.N., 1962: Numerical integration of primitive equations by a quasi-Lagrangian advective scheme. J. Appl.Meteorol., 1, 500-521.

Krishnamurti, T.N., R.J. Pasch and P. Ardanuy, 1980: Prediction of African waves and specification of sqall lines. TELLUS, 32, 215-231.

Lau, N.C., 1984: A comparison of circulation statistics based on FGGE level III-b analyses produced by GFDL and ECMWF for the special observing periods. NOAA Data Report ERL GFDL-6, 237 pp.

Mathur, M.B., 1970: A note on an improved quasi-Lagrangian advective scheme for primitive equations. Mon. Wea. Rev., 98, 214-219.

Matsuno, T., 1966: Numerical integration of primitive equations by a simulated backward difference method. J. Met. Soc. Japan, 44, 76-84.

Neimen, R., 1983: Operational verification of ECMWF forecast field and results for 1980-1981 ECMWF. Tech. Rept. No. 36, 40pp.

Ploshay, J.J., 1977: Results of single level numerical prediction experiments, during GATE. Masters Thesis, Florida State University, Tallahassee, Florida. 32306, USA. 88pp.

Rennick, M.A., 1976: The generation of African waves. J. Atmos. Sci., 33, 1955-1969.

Sanders, F., A.C. Pike and J.P. Gaertner, 1975: A barotropic model for operational prediction of tracks of tropical storms. J. Appl. Meteor., 14, 265-280.

Sanders, F., A.C. Adams, N.J.B. Gordon, and W.D. Jenson, 1980: Further development of a barotropical operational model for predicting paths of tropical storms. Mon Wea. Rev., 108, 642-654.

Shapiro, L., 1977: Tropical storm formation from easterly waves: A criterion for developent. J. Atmos. Sci., 34, 1007-1021.

Tripoli, G. and T.N. Krishnamurti, 1975: Low level flows over GATE area during summer 1972. Mon. Wea. Rev., 103, 197-216.

Williamson, D.L., 1976: Normal mode initialization procedure applied to forecasts with global shallow water equations. Mon. Wea. Rev., 104, 195-206.

Yap, K.S., S. Tint and T.N. Krishnamurti, 1983: Regional single level prediction experiments during winter MONEX, FSU report. Tallahassee, Florida 32306, USA.

END

FILMED

10-85

DTIC